**Title**
Ribonucleases and Their Regulatory Role in Gene Expression



**Author**
Wang, Charles

**Publication Date**
2020

UNIVERSITY OF CALIFORNIA

Los Angeles

# Ribonucleases and Their Regulatory Role in Gene Expression in *Saccharomyces cerevisiae*

A dissertation submitted in partial satisfaction of

the requirements for the degree of Doctor of Philosophy

in Biochemistry and Molecular Biology

by

Charles Wang

2020

ABSTRACT OF THE DISSERTATION

Ribonucleases and Their Regulatory Role in Gene Expression

in *Saccharomyces cerevisiae*

by

Charles Wang

Doctor of Philosophy in Biochemistry and Molecular Biology

University of California, Los Angeles, 2020

Professor Guillaume Chanfreau, Chair

Ribonucleases are essential for the proper biogenesis and turnover of RNAs, and therefore have a major impact on the proper control and fidelity of gene expression. The budding yeast *Saccharomyces cerevisiae* contain various ribonucleases, each with their own specific substrates, specificities and role in RNA metabolism. Due to the complex nature of these ribonucleases, many questions regarding their regulatory role and relative contribution to various cellular pathways remain to be discovered. In this dissertation, we present our findings on two ribonucleases, the exoribonuclease Rrp6p and the RNase III Rnt1p. First, we show a unique regulatory role of Rrp6p for the proper expression of cell wall proteins during heat stress. This process requires the cooperation of the cell wall integrity (CWI) pathway, as demonstrated through the synthetic lethal interaction observed between Rrp6p and CWI factors under heat stress. Strikingly, Rrp6p participates in this pathway independent of its exonuclease activity or association with the nuclear exosome. These results suggest a unique function of Rrp6p and how it contributes to cellular fitness during stress. In chapter 3, we explore the nuclear RNase III Rnt1p and the regulation of its activity under various stresses. Previously, we have shown that

Rnt1p display a drastic increase in cleavage activity towards a select few of its target substrates during high salt stress. However, the mechanism governing this hyperactivation of Rnt1p remains unclear. Here, we show that the salt stress induced hyperactivation of Rnt1p on the substrate RNA of *BDF2* is recapitulated when the processing and export of mRNAs are hindered. This suggests that the activity of Rnt1p can be regulated through the nuclear retention of its RNA substrates. Furthermore, we show that the identity of the Rnt1p recognition stem loop on its target RNAs may affect its cleavage efficiency *in vivo* and *in vitro.* Altogether, this work reveals significant insights on the regulatory role of ribonucleases and how they may contribute to overall cell health.

The dissertation of Charles Wang is approved.

Albert J. Courey

James Akira Wohlschlegel

Guillaume Chanfreau, Committee Chair

University of California, Los Angeles

2020

To my friends and family for their encouragement and support

**TABLE OF CONTENTS** **PAGE**

**LIST OF FIGURES** **PAGE**

**LIST OF SUPPLEMNTARY FIGURES** **PAGE**

**Acknowledgements**

I would like to thank Dr. Guillaume Chanfreau for his tremendous support, unwavering faith and brilliant mentorship. This work would not have been possible without him. His guidance and support have helped me mature and develop lasting skills as a scientist. I am extremely grateful for the opportunity to work with him and I will always treasure our time together.

I would also like to thank my colleagues and friends for their support and friendship and for providing me a work environment I look forward to every day. I would like to especially thank Jason Gabunilas, a close friend for whom I have had a pleasure of working with during most of my graduate career. Our thoughtful and intellectual conversations have helped me develop as a scientist throughout the many years. I am also heavily indebted to Kevin Roy and grateful for his guidance and encouragement during my first few years of graduate school. He has paved the foundation for my work in Chapter 3 and it would have not been possible without him. I would also like to thank Domi Hodko, who I owe tremendously for his time and dedication in my initial training within the lab. His mentorship in yeast work and experimental biology has laid the groundwork for the rest of my graduate career.

I am extremely grateful for all the undergraduate research assistants that I have worked with. Their extensive dedication and support were indispensable towards my work here at UCLA. I would like to especially recognize Yanrui (Cindy) Liu and Indya Weathers for their relentless efforts and assistance with Chapter 2, and Carlos Gonzalez for his assistance and contributions with Chapter 2 and 3. I would like to thank our lab assistant Martina Rivas for tirelessly keeping the lab running smoothly and efficiently.

Outside of the laboratory, I am very fortunate for the friendships and bonds that were formed over the years. I would like to especially acknowledge Sam Han, Sue Tsui, Eric Torres and Kelly Quinn for their exceptional friendship and support. I will always cherish the time we have spent together. I am also heavily indebted and grateful for my family, especially to my

grandparents, parents and brothers who have encouraged and supported me throughout my life.

Reprint of Publications

Wang, C., Liu, Y., DeMario, S., Mandric, I., Gonzalez-Figueroa, C., and Chanfreau, G. Rrp6 moonlights in a role that is independent of the RNA exosome to synergize with the functions of the cell wall integrity factors Slt2/Mpk1 and Paf1 during heat stress. Submitted.

Chapter 2 is a submitted manuscript, with the majority of the work performed by me. Sam DeMario and Igor Mandric were essential for the bioinformatic analysis of the RNA-Seq data. I am also grateful to Carlos Gonzalez-Figueroa who contributed to Figure 2, and Yanru Liu who contributed to Figure S2 and assisted in many of the experiments in this manuscript. This manuscript was written by me and the principal investigator Guillaume Chanfreau.

Chapter 3 is a manuscript in preparation. This work is a continuation of Kevin Roy's work on Rnt1p and would not be possible without his initial studies. The majority of the work was performed by me and the manuscript was written with the principal investigator Guillaume Chanfreau. I am indebted to Carlos Gonzalez-Figueroa for his technical assistance in this chapter.

Funding sources

Ruth L. Kirschstein National Research Service Award GM007185 (2015-2018)

## VITA

### Education

2013 B.S. in Biochemistry/Chemistry
University of California, San Diego

### Publications

**Wang, C.**, Liu, Y., DeMario S., Mandric, I., Gonzalez-Figueroa, C., and Chanfreau, G. Rrp6 moonlights independently from the exosome to synergize the functions of Mpk1 and Paf1 during heat stress. **Submitted.**

White, J. T., Cato, T., Deramchi, N., Gabunilas, J., Roy, K., **Wang, C**., Chanfreau, G., Clarke, S. G. (2019). Protein methylation and translation: Role of lysine modification on the function of yeast elongation factor 1A. Biochemistry, acs.biochem.9b00818. https://doi.org/10.1021/acs.biochem.9b00818

He, C.H., Black, D.S., Nguyen, T.P.T., **Wang, C.**, Srinivasan, C., and Clarke, C.F. (2015). Yeast Coq9 controls deamination of coenzyme Q intermediates that derive from para-aminobenzoic acid. Biochim. **Biophys. Acta - Mol. Cell Biol**. Lipids *1851*, 1227–1239.

Allan, C.M., Awad, A.M., Johnson, J.S., Shirasaki, D.I., **Wang, C.**, Blaby-Haas, C.E., Merchant, S.S., Loo, J.A., and Clarke, C.F. (2015). Identification of Coq11, a New Coenzyme Q Biosynthetic Protein in the CoQ-Synthome in *Saccharomyces cerevisiae*. **J. Biol. Chem**. *290*, 7517–7534.

Tamir, S., Rotem-Bamberger, S., Katz, C., Morcos, F., Hailey, K.L., Zuris, J.A., **Wang, C.**, Conlan, A.R., Lipper, C.H., Paddock, M.L., et al. (2014). Integrated strategy reveals the protein interface between cancer targets Bcl-2 and NAF-1. **Proc. Natl. Acad. Sci**. *111*, 5177–5182.

Baxter, E.L., Zuris, J.A., **Wang, C.**, Vo, P.L.T., Axelrod, H.L., Cohen, A.E., Paddock, M.L., Nechushtai, R., Onuchic, J.N., and Jennings, P.A. (2013). Allosteric control in a metalloprotein dramatically alters function. Proc. **Natl. Acad. Sci**. *110*, 948–953.

### Seminars and poster presentations

The nuclear exosome component Rrp6 synergizes with the Mpk1 and Paf1 elongation factors for proper gene expression during stress response . Jonsson Comprehensive Cancer Center Epigenomics, RNA and Gene Regulation Group Meeting, UCLA, CA. [Seminar]. Nov 2019

The Nuclear Exosome Independent Function of Rrp6 in Promoting Cell Survival Under Stress. RNA 2018, Berkeley, CA. [Poster presentation]. May 2018

*BDF2* Transcript Sensitivity to RNase III Mediated Decay is Heavily Governed by Transcript Localization and Structural Context. RNA 2017, Czech Republic. [Poster presentation]. May 2017

BDF2 Transcript Sensitivity to RNase III Mediated Decay is Heavily Governed by Transcript Localization and Structural Context. American Society for Biochemistry and Molecular Biology (ASBMB), Chicago, IL. [Poster presentation]. April 2017

**Awards**

| | |
|---|---|
| Ruth L. Kirschstein National Research Service Award GM007185<br>The Cellular and Molecular Biology Training Grant ($70,000) | 2015-2018 |
| UC San Diego Physical Sciences Dean's Undergraduate Award for Excellence | 2013 |

Chapter 1

# Introduction to RNA regulation and quality control in *Saccharomyces cerevisiae*

**RNA regulation and quality control**

All eukaryotes including the budding yeast, *S. cerevisiae*, rely on the fundamental ability to control the expression of its genetic material for proper development and stress adaption. Due to its large impact on cellular fitness, all aspects of gene expression must be regulated, from the transcription of specific genes to the post translational modification of the gene product (Figure 1.1). Ribonucleic acids (RNAs) act as an intermediary of gene expression as all genetic material must be conveyed through its corresponding RNA. This provides a key area to precisely coordinate the expression of genes through the modulation of RNA processing, export or stability. These processes often work in concert to add an additional layer of complexity in the determination of RNA fate. One classical example of a synergistic approach for regulating RNA is the coupling of splicing to RNA decay pathways (Kawashima et al., 2009; Roy and Chanfreau, 2014; Volanakis et al., 2013). Extensive studies have also revealed that specific proteins may auto-regulate their own RNA transcripts to fine-tune their own expression (Gabunilas and Chanfreau, 2016). As a result of these comprehensive and diverse regulatory pathways, only a fraction of precursor RNAs become fully mature and functional (Mata et al., 2005).

Over 900 genes are upregulated or suppressed in response to specific environmental growth conditions in *S. cerevisiae* (Gasch, 2003). This response leads to a drastic change in the transcriptome, with each RNA transcript heavily monitored for its integrity, abundance, and function. Aberrant RNAs may be produced during any step of RNA biogenesis, beginning with the inherent error rate of transcription to the improper ribonucleoprotein assembly of RNAs. This necessitates multiple quality control mechanisms to remove faulty and nonfunctional RNAs. Defects within these quality control pathways have been attributed to many human diseases and disorders (Moraes, 2010). In the last few decades, in depth studies in *S. cerevisiae* have uncovered a repertoire of quality control mechanisms and their relative contribution to cellular fitness. These pathways include no-go decay (NGD), Rnt1p mediated decay (RMD) and non-sense mediated decay (NMD) (Chang et al., 2007; Doma and Parker, 2006; Klauer and van

Hoof). These multiple quality control pathways have evolved to preferentially target and remove aberrant RNAs. In addition, quality control pathways often play a regulatory role as well, where functional but undesirable RNAs are selectively targeted for degradation (Mühlemann and Jensen, 2012). The utilization of quality control pathways to degrade functional RNAs creates a constant kinetic competition between RNA biogenesis and turnover (Mühlemann and Jensen, 2012). This balance gives the cell the ability to rapidly shift and alter gene expression according to its needs.

**RNA decay by the nuclear exosome**

The nuclear exosome complex is the primary machinery involved in the 3' to 5' exo- and endo-nucleolytic degradation or processing of nuclear RNAs. It is believed that all classes of RNA are effected by the nuclear exosome, from their biogenesis to decay (Figure 1.2) (Kilchert et al., 2016). As so, the nuclear exosome plays a large role in regulating gene expression through modulating functional RNA transcript availability. In addition, its effect on ribosomal RNA (rRNA) processing directly effects polypeptide synthesis and protein abundance (Ghosh and Jacobson, 2010). Due to its large contribution to diverse biological processes, the nuclear exosome is a highly conserved and essential complex (Lykke-Andersen et al., 2009). Several human disorders and cancers have been attributed to mutations within the nuclear exosome, including myelogenous leukemia, pontocerebellar hypoplasia, spinal neuron degeneration and retinitis pigmentosa (Fasken et al., 2017; Gillespie et al., 2017; Morton et al., 2018; Staals and Pruijn, 2010; Wan et al., 2012)..

The nuclear exosome was first discovered in 1996 as a central factor in rRNA processing (Mitchell et al., 1996). A genetic screening identified Rrp4p as a necessary component in the processing of the 7s pre-rRNA through an exonuclease mechanism (Mitchell et al., 1996). Subsequent analysis identified that Rrp4p exists in a complex, termed the exosome, with Rrp41p, Rrp42p, Rrp43p and Rrp44p (Dis3P) (Mitchell et al., 1997). All four of

these proteins were structurally related to the 3' to 5' exoribonucleases of *E. coli*; Rrp41p, Rrp42p and Rrp43p belong in the RNase PH family of exoribonucleases, whereas Rrp44p shared homology with RNase II (Mitchell et al., 1997). These structural similarities towards known exoribonucleases further corroborated the exonuclease function of the newly discovered exosome. In 1999, mass spectrometry analysis identified the remaining exosome complex components as Rrp40p, Rrp45p, Rrp46p, Rrp6p, Csl4p and Mtr3p (Allmang et al., 1999). Mtr3p, Rrp45p and Rrp46p are homologous to *E.coli* RNase PH, whereas Rrp6p is homologous to *E.coli* RNase D (Allmang et al., 1999). Mutations within select components of the exosome inhibited rRNA processing and hindered mRNA turnover (Anderson et al., 1998). Both Rrp6p and Rrp44p display nuclease activities (Kilchert et al., 2016).

It was a decade later until the first structure of the eukaryotic RNA exosome was determined through x-ray crystallography (Liu et al., 2006). A simplified depiction is shown in Figure 1.3A. The RNA exosome consists of a barrel-like core containing the RNase PH-like proteins: Rrp41p, Rrp42p, Rrp43p, Rrp45p and Rrp46p (Kilchert et al., 2016). The core contains a channel just large enough to accommodate a single stranded RNA (Liu et al., 2006). The lid of the barrel consists of Rrp4p, Rrp40p and Csl1p (Kilchert et al., 2016). The nuclear nine-subunit core (EXO9) associates with two hydrolytic exoribonuclease proteins; Rrp6p near the top of the barrel, and Dis3p near the bottom (Buttner et al., 2006; Kilchert et al., 2016). Rrp6p binds directly to Rrp47p, which aids in the recruitment of Mtr4p and the processing of RNAs (Garland et al., 2013; Schuch et al., 2014).

Due to the relative position of Dis3p, RNAs targeted for degradation are threaded through the barrel to access its active site (Figure 1.3B) (Schneider and Tollervey, 2013). In addition, a conformational change of Dis3p may further allow direct access of RNAs to its active site without the need to enter through the central channel (Figure 1.3C) (Han and Van Hoof, 2016). It is unclear how RNAs reach Rrp6p *in vivo*. It has been proposed that RNAs may directly reach Rrp6p without interacting with any other exosome units (Figure 1.3D). Indeed, research

have shown that a core exosome-independent Rrp6 mutant still retains its function on specific RNA substrates (Callahan and Butler, 2008). In addition, more recent structure analysis suggests that RNAs can be threaded between the cap and barrel to reach Rrp6 (Figure 1.3E) (Wasmuth et al., 2014). The proposed routes are not mutually exclusive and may depend largely on the RNA's structure, binding proteins and adapters. (Wasmuth et al., 2014). In contrast to the nuclear exosome, the cytoplasmic exosome does not contain Rrp6p. Instead, the interaction between the exosome and Ski7p is thought to facilitate the degradation of specific RNAs (Liu et al., 2016).

**Selective decay by the nuclear exosome**

The nuclear exosome is extremely versatile in its involvement in RNA synthesis, maturation and turnover. The ability of the exosome to distinguish between a wide range of RNA substrates relies on several exosome-associated factors and complexes. In fact, purified exosome complexes have weak activities *in vitro* as they lack these protein partners (Kilchert et al., 2016; LaCava et al., 2005). Helicases are one of the most important cofactors of the nuclear exosome, as the RNA must be unstructured to be threaded through the 8-10 angstrom narrow channel of its core (Liu et al., 2006). These helicases include the DExH-box Mtr4p within the nucleus, and the super killer Ski2p within the cytoplasm (Kilchert et al., 2016).

Mtr4p is found within the TRAMP complex, a large contributor of RNA substrates for the nuclear exosome. The TRAMP complex consists of the RNA binding protein Air1p or Air2p, the non-canonical poly(A) polymerase Trf4p or Trf5p and the DExH-box helicase Mtr4p (Figure 1.4) (Ghosh and Jacobson, 2010; LaCava et al., 2005). These proteins work in concert to recognize RNA substrates and prepare them for degradation by the nuclear exosome. Air1p or Air2p first binds to its target RNA, whereby Trf4p or Trf5p initiates the addition of a short poly(A) tail (Ghosh and Jacobson, 2010; Kilchert et al., 2016). This tail facilitates the binding of Mtr4 to unwind RNA secondary structures and to recruit the nuclear exosome for subsequent RNA

hydrolysis (Ghosh and Jacobson, 2010; Kilchert et al., 2016). The short poly(A) tail also provides the exosome with an unstructured RNA 3' end to initiate degradation (Ghosh and Jacobson, 2010). This contrasts with the much longer and protective poly(A) tails produced by the canonical polyadenylation complex.

The TRAMP complex itself is largely unspecific and may polyadenylate all RNAs with accessible 3' ends. In this way, the TRAMP complex acts as a surveillance pathway that targets unprotected RNAs for degradation (Lykke-Andersen et al., 2009). These RNA substrates may include hypomodified tRNAs, improperly processed noncoding and coding RNAs, and RNA cleavage products from various RNases (Lykke-Andersen et al., 2009; Roy and Chanfreau, 2014). In addition, the TRAMP complex also functions in directing RNAs to the nuclear exosome for processing. Therefore, the TRAMP complex must be able to distinguish between RNAs that require processing or degradation - a role usually fulfilled through various cofactors and RNA binding proteins (Callahan and Butler, 2010). For example, both Utp18p and Nop53p are shown to bind to a conserved arch interaction motif (AIM) within rRNA intermediates, and recruit the TRAMP complex through its interaction with Mtr4p (Thoms et al., 2015). While Nop53p targets rRNA to be processed by the exosome, Utp18p targets them for degradation (Thoms et al., 2015; Zinder and Lima, 2017). The differences in the fate of these substrates are largely attributed to the action of their respective binding proteins. Specific RNA binding proteins, such as Nop53p, may physically impede the nuclear exosome and result in a partially digested and processed RNA (Kilchert et al., 2016). Altogether, the TRAMP complex plays the essential role of RNA recognition and preparation for the nuclear exosome. Due to its pivotal role, the TRAMP complex has been shown to regulate Pol II elongation, silence genes, and to maintain genome integrity (Gavaldá et al., 2013; Wang et al., 2008).

The action of the TRAMP complex can be coupled with RNA termination through the trimeric NNS complex consisting of Nrd1p, Nab3p and Sen1 (Tudek et al., 2014). The NNS complex terminates cryptic pervasive transcripts, noncoding RNAs, as well as some coding

RNAs as a method to regulate their expression (Arndt and Reines, 2015). These NNS substrates contain binding motifs that Nrd1p or Nab3p would recognize. The helicase Sen1 is then thought to pull the nascent RNA out of the active site of the polymerase and thereby collapse the transcription bubble (Arndt and Reines, 2015). The resulting terminated RNA transcripts are targeted for degradation or processing through the TRAMP complex. A kinetic competition between the NNS complex and either elongation factors or termination factors determines the outcome of some coding RNAs (Mühlemann and Jensen, 2012). Interestingly, NNS induced termination may also act as a fail-safe mechanism for transcripts that fail to terminate at its proper site (Lemay and Bachand, 2015). Transcripts that escape polyadenylation by the canonical polyadenylation complex are instead polyadenylated by the TRAMP complex for degradation by the nuclear exosome (Lemay and Bachand, 2015). In this manner, the nuclear exosome is indirectly involved in the quality control of improperly terminated and processed RNAs.

**Rnt1p mediated decay and processing of nuclear RNAs**

Cleavage of double stranded RNAs (dsRNAs) is an essential process for the maturation and degradation of many RNA transcripts. Rnt1p is the only double-stranded specific endoribonuclease found within *S. cerevisiae* and was originally identified through its sequence homology to bacterial RNase III (Bernstein et al., 2012; Kufel et al., 1999). The structure of Rnt1p is simple, as it only contains four domains: an N-terminal domain (N-Ter), a nuclease domain (NucD), a double-stranded RNA binding domain (dsRBD) and a nuclear localization signal (NLS) in its C-terminal domain (C-Ter) (Figure 1.5A). This RNA binding domain recognizes any tetraloops that adopts an AGNN tetraloop conformation (Figure 1.5B) (Rondón et al., 2009). This results in the dimerization of the Rnt1p enzyme and the subsequent cleavage of the dsRNA 14-16 nucleotides away from the loop (Rondón et al., 2009). The nuclease domain contains multiple conserved amino acids for the coordination of 2 $Mg^{2+}$ ions necessary

for its RNase activity (Bernstein et al., 2012). These bivalent metal ions aid in the hydrolysis of phosphodiester bonds within RNA, resulting in a 5'-phosphate and a 3'-hydroxyl RNA product (Meng and Nicholson, 2008). The unprotected 3'-hydroxyl RNA cleavage product is subsequently recognized by TRAMP and the nuclear exosome for processing or degradation. In this fashion, Rnt1p plays a significant role in the processing and turnover of specific nuclear RNAs. The absence of Rnt1p results in a severe slow growth phenotype and an extreme sensitivity to multiple stresses (Catala et al., 2012; Elela and Ares, 1998).

Rnt1p was first identified for its role in the initial step of ribosomal RNA processing in yeast (Kufel et al., 1999). A classical Rnt1 recognition tetraloop is present within the 3' external transcribed region of the 35s pre-rRNA and initiates the termination of the polymerase and the release of the 35s pre-rRNA for further processing. The recognition and cleavage of the rRNA precursor occurs co-transcriptionally, as Rnt1p has been found to localize at the site of transcription (Henras et al., 2004). Although the proper biogenesis of rRNA is critical for yeast, the absence of Rnt1p is not lethal despite its slow growth phenotype. This is due to a failsafe mechanism found downstream of the Rnt1p recognition stem loop responsible for the termination and release of an extended 35s precursor transcript (Braglia et al., 2011). Further studies revealed that Rnt1p is also involved in the processing of snoRNAs and snRNAs by coupling RNA cleavage to its trimming by exonucleases (Chanfreau, 1998; Elela and Ares, 1998; Henras et al., 2005). Typically, snoRNAs rely on Rnt1p mediated cleavage of its RNA to allow an entry site for the 5' processing of the RNA by the exonuclease Rat1p. On the other hand, snRNAs usually utilizes Rnt1p as a method to trim its 3'end through the nuclear exosome. The exact type of processing these noncoding RNAs undergo largely depend on its associated proteins and the location of the Rnt1 cleavage site (RCS) within the precursor RNAs. The proper processing of these noncoding RNAs is particularly important as they are involved in the splicing or modification of RNAs within the cell.

**A regulatory role of Rnt1p**

Rnt1p has long been thought to only target nuclear noncoding RNAs for cleavage and processing. However, evidence has uncovered a relatively new role of Rnt1p in the surveillance and regulation of coding RNAs. This process can be coupled with other degradative pathways to limit improperly processed or unnecessary RNAs. For example, Rnt1p cleavage may act as a fail-safe mechanism for RNAs that failed to terminate at the proper location due to weak polyadenylation (pA) signals (Ghazal et al.; Rondón et al., 2009). Based on the relative location of the RCS to the pA site, the RNAs are either degraded by the nuclear exosome or processed to become a fully functional RNA (Rondón et al., 2009). Rnt1p may also compete with other processing factors for its RNA substrates. One such example is the competition between Rnt1p and the spliceosome complex towards RNAs containing an RCS within its intronic region. Changes in growth conditions may shift the competition in favor of one process over the other. Conditions that promote Rnt1p activity lead to a decrease in RNA transcript abundance and a repression of the gene's expression. In contrast, conditions which promote splicing would lead to an increase in the abundance of mature RNA transcript. This constant competition enables the cell to fine tune the expression of these transcripts.

In depth computational and biochemical work have identified hundreds of coding and noncoding RNAs targeted by Rnt1p (Gagnon et al., 2015). The cleavage of each RNA by Rnt1p is tightly controlled to regulate its stability and expression. Interestingly, the identity of the RCS itself may regulate the activity of Rnt1p on the transcript (Comeau et al., 2016). RCS with unpaired nucleotide ends are highly reactive substrates for Rnt1p, resulting in a higher catalytic efficiency and turnover rate. These unpaired nucleotides within the RCS are thought to destabilize the catalytic complex to trigger product release (Comeau et al., 2016). A majority of highly reactive Rnt1p substrates are found to be non-coding RNAs (Comeau et al., 2016). These substrates have evolved to undergo rapid cleavage for further downstream processing. Coding RNAs, on the other hand, tend to be less efficient Rnt1p substrates as their RCS tend to

contain paired nucleotide ends that decrease the product release rate (Comeau et al., 2016). This gives the opportunity for other factors to modulate the processing or stability of the transcript. Altogether, Rnt1p plays a largely underappreciated role in the processing and regulation of nuclear RNAs.

**Gene regulation through RNA localization**

Spatial gene regulation plays a significant role in determining the fate of RNAs (Singer-Krüger and Jansen, 2014). The selective localization of RNAs within various organelles affects their ability to be translated and/or degraded (Singer-Krüger and Jansen, 2014). Specific trafficking pathways are involved in determining the localization of RNAs, targeting the RNAs towards the nucleus, mitochondria, endoplasmic reticulum (ER) or other cellular compartments (Singer-Krüger and Jansen, 2014). Proteins involved in these pathways recognize and bind to specific cis elements within RNAs, often co-transcriptionally, and regulates their transport within the cell (Singer-Krüger and Jansen, 2014). These diverse cis elements are often found within the 3' untranslated regions (UTRs) of RNAs (Singer-Krüger and Jansen, 2014).

The cytoplasmic export of mRNAs is crucial for the expression of genes. The separation of region between RNA synthesis and translation requires the export of mRNAs between the nucleus and cytoplasm (Hammell et al., 2002). This offers an opportunity for the regulation of RNAs. For example, heat shock or ethanol stress results in the selective nuclear retention of bulk poly(A)+ mRNAs, while mRNAs of heat shock genes are freely exported to the cytoplasm for translation (Izawa et al., 2008; Saavedra et al., 1996, 1997). This process enables the quick expression of heat shock proteins for a rapid adaption to the cellular stress. As so, the selective nuclear retention of mRNAs may be used as a method to regulate the expression of specific mRNAs.

In addition to affecting the translation of RNAs, the localization of RNAs is often used for their quality control as well. The export of RNAs is tightly coupled to its 3' -end processing,

whereby improperly processed RNAs are sequestered within the nucleus for further processing or degradation (Hammell et al., 2002). These retained RNAs may be sequestered at the site of transcription, within the nucleolus, or at the nuclear pore based on the type of disruption (Paul and Montpetit, 2016). Improperly processed RNAs are often substrates for the nuclear exosome due to a lack of a protective poly(A) tail. Altogether, this process ensures that only competent RNAs are exported and translated in the cytoplasm.

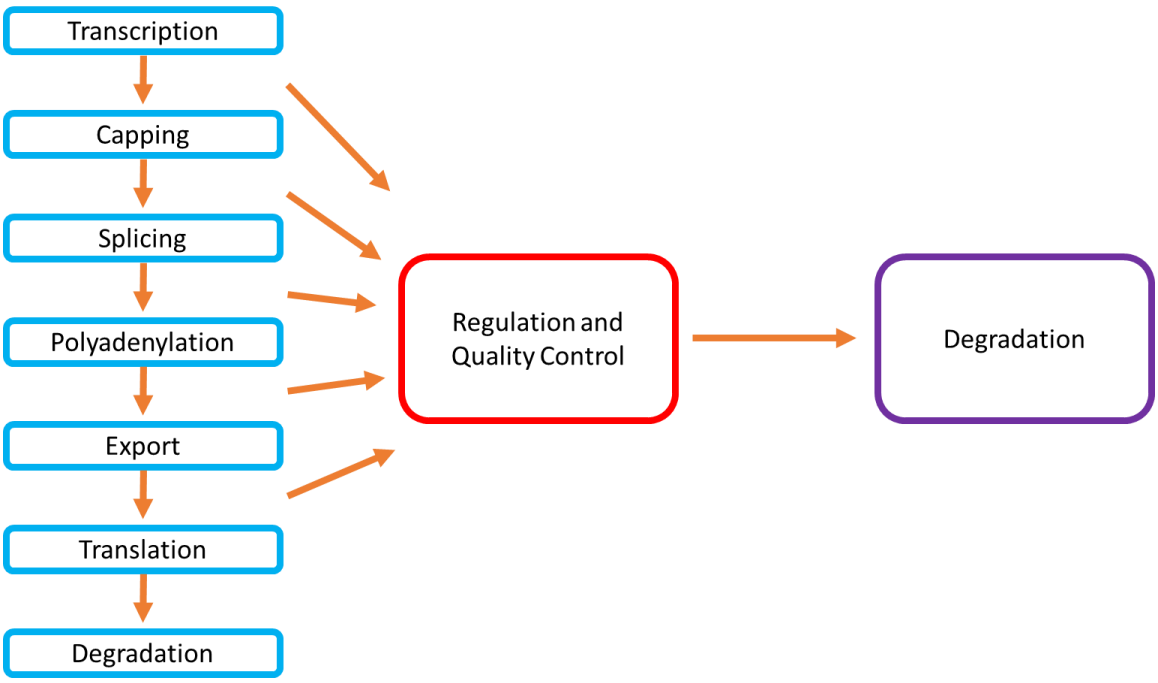


**Figure 1.1. Regulation and quality control of gene expression.** The expression of genes requires a multistep pathway that is heavily regulated during each process. Aberrant RNAs and proteins are rapidly degraded through various quality control pathways to ensure the fidelity of gene expression.

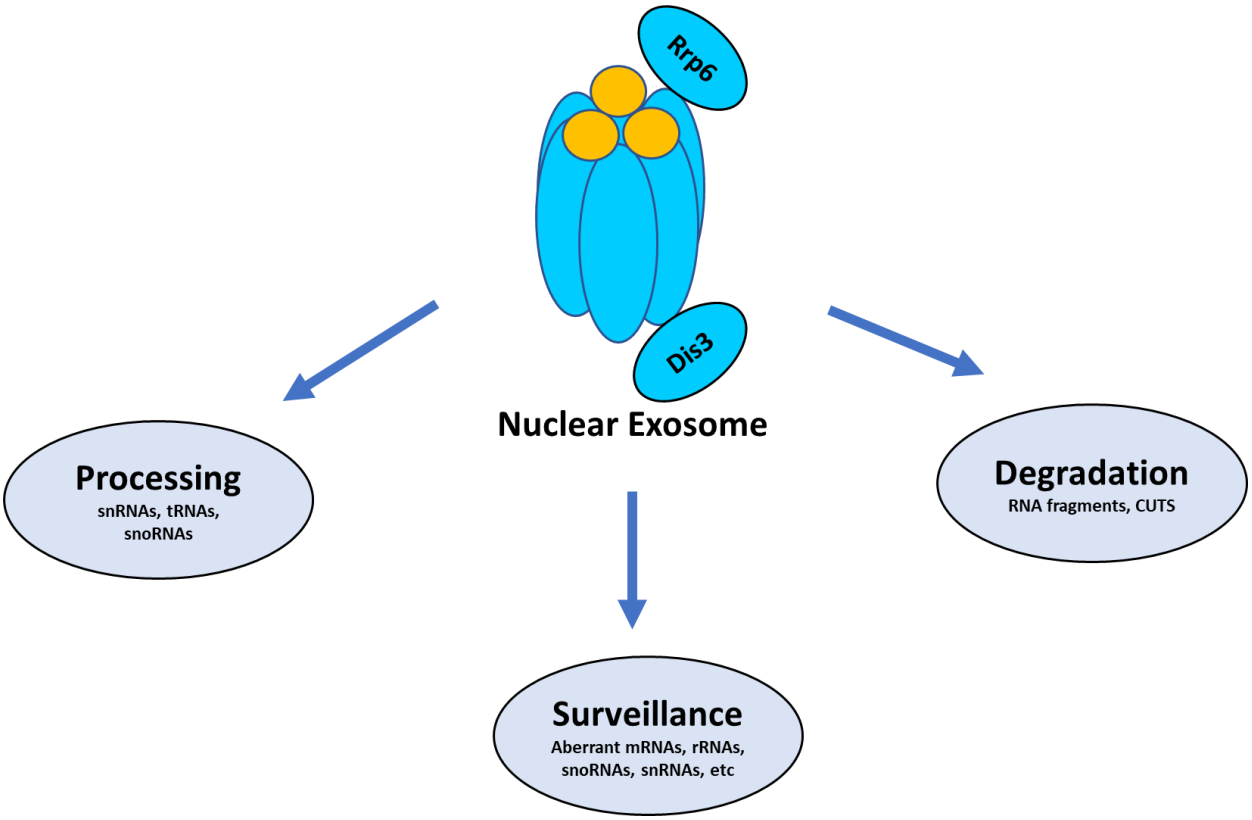


**Figure 1.2. The nuclear exosome is involved in many aspects of RNA biogenesis and decay.** Various RNAs of all classes require the nuclear exosome for proper processing, surveillance and degradation.

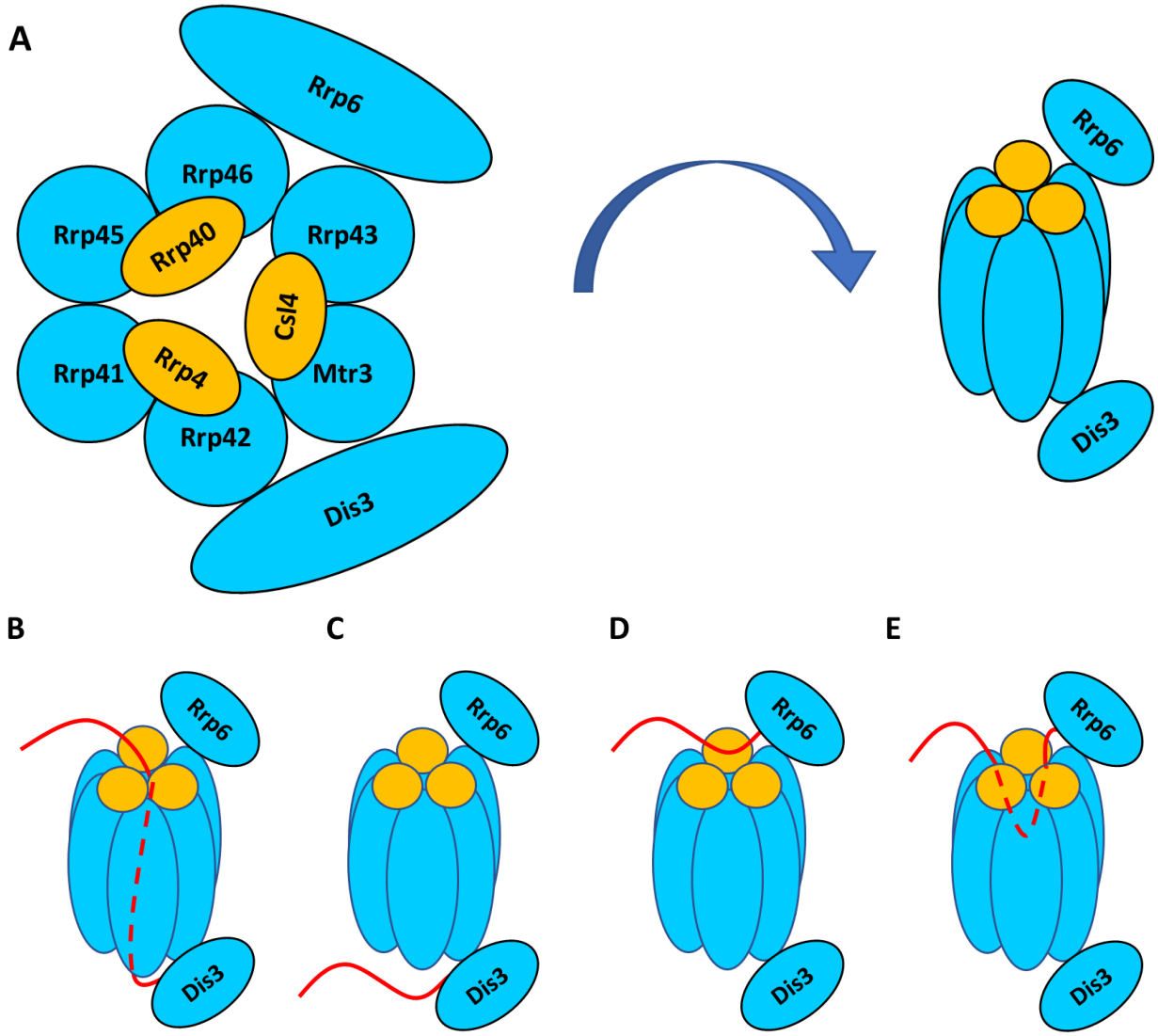


**Figure 1.3. Simplified structure of the nuclear exosome and the routes RNAs may take to reach the active sites. A.** The nuclear exosome consists of 6 proteins forming a barrel-like core and 3 proteins forming a cap-like structure. Rrp6p and Dis3p associates with the complex and provides its exonuclease activities. To reach Dis3p, RNA substrates are either (**B**) threaded through the core or (**C**) a conformational change of Dis3p allows RNA direct access. Similarly, RNA substrates of Rrp6p can be (**D**) threaded through the core or (**E**) directly access Rrp6p. RNA binding proteins and exosome cofactors often determine the fate of the RNA substrates.

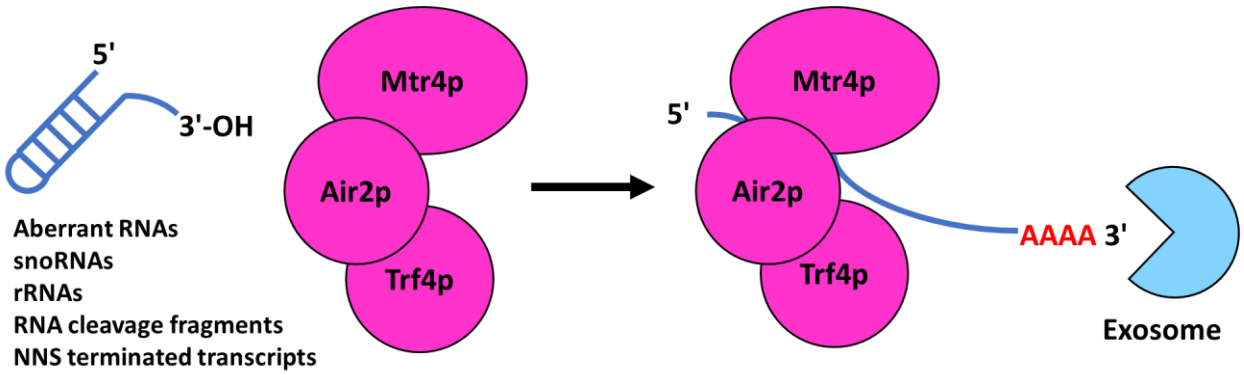


**Figure 1.4. The TRAMP complex is a major contributor of RNA substrates for the nuclear exosome.** The TRAMP complex targets a variety of RNA substrates to the nuclear exosome for processing or degradation. RNA substrates are unwound by the Mtr4p helicase to remove secondary structures, and oligo-adenylated to promote binding to the nuclear exosome.

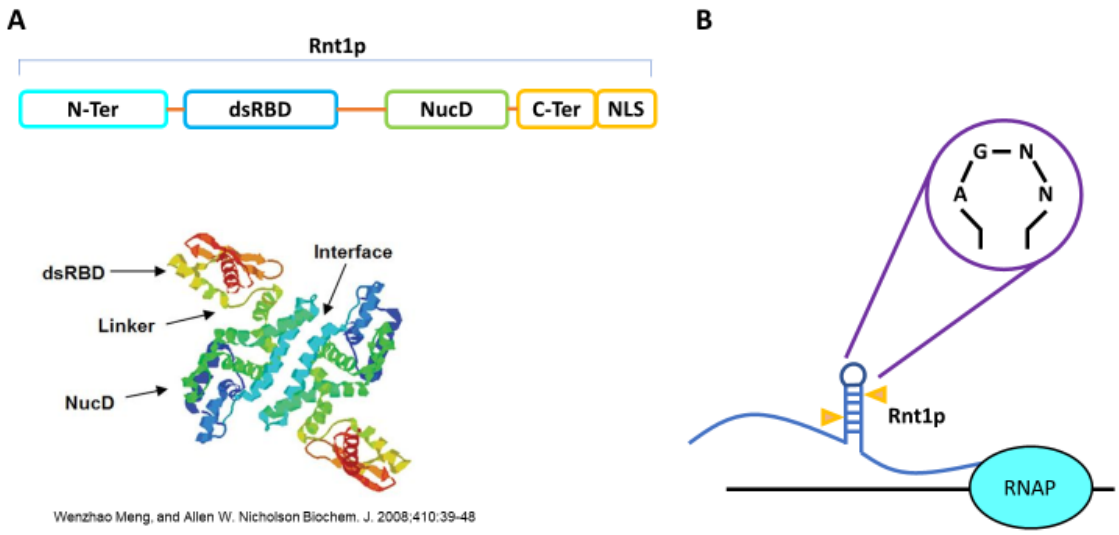


**Figure 1.5. Structure of Rnt1p and its substrate recognition site. A.** Rnt1p consists of an N-terminal domain (N-Ter), nuclease D domain (NucD), a double stranded RNA binding domain (dsRBD) and a C-terminal domain (C-Ter) that contains a nuclear localization signal (NLS). Rnt1p is active as a homodimer. **B.** Rnt1p recognizes RNA substrates containing an AGNN tetraloop (or tetraloops with similar structural conformation) and introduces two staggered cuts along the stem loop.

## References


Allmang, C., Petfalski, E., Podtelejnikov, A., Mann, M., Tollervey, D., and Mitchell, P. (1999). The yeast exosome and human PM-Scl are related complexes of 3’ --> 5’ exonucleases. Genes Dev. *13*, 2148–2158.

Anderson, J.S.J., Parker, R.P., Basilion, J.P., Koeller, D.M., Klausner, R.D., and Harford, J.B. (1998). The 3’ to 5’ degradation of yeast mRNAs is a general mechanism for mRNA turnover that requires the SKI2 DEVH box protein and 3’ to 5’ exonucleases of the exosome complex. EMBO J. *17*, 1497–1506.

Arndt, K.M., and Reines, D. (2015). Termination of Transcription of Short Noncoding RNAs by RNA Polymerase II. Annu. Rev. Biochem. *84*, 381–404.

Bernstein, D.A., Vyas, V.K., and Fink, G.R. (2012). Genes come and go: the evolutionarily plastic path of budding yeast RNase III enzymes. RNA Biol. *9*, 1123–1128.

Braglia, P., Kawauchi, J., and Proudfoot, N.J. (2011). Co-transcriptional RNA cleavage provides a failsafe termination mechanism for yeast RNA polymerase I. Nucleic Acids Res. *39*, 1439–1448.

Buttner, K., Wenig, K., and Hopfner, K.-P. (2006). The exosome: a macromolecular cage for controlled RNA degradation. Mol. Microbiol. *61*, 1372–1379.

Callahan, K.P., and Butler, J.S. (2008). Evidence for core exosome independent function of the nuclear exoribonuclease Rrp6p. Nucleic Acids Res. *36*, 6645–6655.

Callahan, K.P., and Butler, J.S. (2010). TRAMP complex enhances RNA degradation by the nuclear exosome component Rrp6. J. Biol. Chem. *285*, 3540–3547.

Catala, M., Aksouh, L., and Abou Elela, S. (2012). RNA-dependent regulation of the cell wall stress response. Nucleic Acids Res. *40*, 7507–7517.

Chanfreau, G. (1998). Processing of a dicistronic small nucleolar RNA precursor by the RNA endonuclease Rnt1. EMBO J. *17*, 3726–3737.

Chang, Y.-F., Imam, J.S., and Wilkinson, M.F. (2007). The nonsense-mediated decay RNA surveillance pathway. Annu. Rev. Biochem. *76*, 51–74.

Comeau, M.-A., Lafontaine, D.A., and Abou Elela, S. (2016). The catalytic efficiency of yeast ribonuclease III depends on substrate specific product release rate. Nucleic Acids Res. *44*, 7911–7921.

Doma, M.K., and Parker, R. (2006). Endonucleolytic cleavage of eukaryotic mRNAs with stalls in translation elongation. Nature *440*, 561–564.

Elela, S.A., and Ares, M. (1998). Depletion of yeast RNase III blocks correct U2 3' end formation and results in polyadenylated but functional U2 snRNA. EMBO J. *17*, 3738–3746.

Fasken, M.B., Losh, J.S., Leung, S.W., Brutus, S., Avin, B., Vaught, J.C., Potter-Birriel, J., Craig, T., Conn, G.L., Mills-Lujan, K., et al. (2017). Insight into the RNA Exosome Complex Through Modeling Pontocerebellar Hypoplasia Type 1b Disease Mutations in Yeast. Genetics *205*, 221–237.

Gabunilas, J., and Chanfreau, G. (2016). Splicing-Mediated Autoregulation Modulates Rpl22p Expression in Saccharomyces cerevisiae. PLoS Genet. *12*, e1005999.

Gagnon, J., Lavoie, M., Catala, M., Malenfant, F., and Elela, S.A. (2015). Transcriptome Wide Annotation of Eukaryotic RNase III Reactivity and Degradation Signals. PLoS Genet. *11*, 1–29.

Garland, W., Feigenbutz, M., Turner, M., and Mitchell, P. (2013). Rrp47 functions in RNA surveillance and stable RNA processing when divorced from the exoribonuclease and exosome-binding domains of Rrp6. RNA *19*, 1659–1668.

Gasch, A.P. (2003). The environmental stress response: a common yeast response to diverse environmental stresses. In Yeast Stress Responses, (Berlin, Heidelberg: Springer Berlin Heidelberg), pp. 11–70.

Gavaldá, S., Gallardo, M., Luna, R., and Aguilera, A. (2013). R-Loop Mediated Transcription-Associated Recombination in trf4Δ Mutants Reveals New Links between RNA Surveillance and Genome Integrity. PLoS One *8*, e65541.

Ghazal, G., Gagnon, J., Jacques, T., Landry, J.-R., ois Robert, F., and Abou Elela, S. Yeast RNase III Triggers Polyadenylation-Independent Transcription Termination. Mol. Cell *36*, 99–109.

Ghosh, S., and Jacobson, A. (2010). RNA decay modulates gene expression and controls its fidelity. Wiley Interdiscip. Rev. RNA *1*, 351–361.

Gillespie, A., Gabunilas, J., Jen, J.C., and Chanfreau, G.F. (2017). Mutations of EXOSC3/Rrp40p associated with neurological diseases impact ribosomal RNA processing functions of the exosome in S. cerevisiae. RNA *23*, 466–472.

Hammell, C.M., Gross, S., Zenklusen, D., Heath, C. V., Stutz, F., Moore, C., and Cole, C.N. (2002). Coupling of Termination, 3' Processing, and mRNA Export. Mol. Cell. Biol. *22*, 6441–6457.

Han, J., and Van Hoof, A. (2016). The RNA exosome channeling and direct access conformations have distinct in vivo functions HHS Public Access. Cell Rep *16*, 3348–3358.

Henras, A.K., Bertrand, E., and Chanfreau, G. (2004). A cotranscriptional model for 3'-end processing of the Saccharomyces cerevisiae pre-ribosomal RNA precursor. RNA *10*, 1572–1585.

Henras, A.K., Sam, M., Hiley, S.L., Wu, H., Hughes, T.R., Feigon, J., and Chanfreau, G.F. (2005). Biochemical and genomic analysis of substrate recognition by the double-stranded RNA binding domain of yeast RNase III. RNA *11*, 1225–1237.

Izawa, S., Kita, T., Ikeda, K., Inoue, Y., Piper, P., Tani, T., Derby, R.J., Hiraoka, Y., Spector, D.L., Saavedra, C., et al. (2008). Heat shock and ethanol stress provoke distinctly different responses in 3′-processing and nuclear export of *HSP* mRNA in *Saccharomyces cerevisiae*. Biochem. J. *414*, 111–119.

Kawashima, T., Pellegrini, M., and Chanfreau, G.F. (2009). Nonsense-mediated mRNA decay mutes the splicing defects of spliceosome component mutations. RNA *15*, 2236–2247.

Kilchert, C., Wittmann, S., and Vasiljeva, L. (2016). The regulation and functions of the nuclear

RNA exosome complex. Nat. Rev. Mol. Cell Biol. *17*, 227–239.

Klauer, A.A., and van Hoof, A. Degradation of mRNAs that lack a stop codon: a decade of nonstop progress. Wiley Interdiscip. Rev. RNA *3*, 649–660.

Kufel, J., Dichtl, B., and Tollervey, D. (1999). Yeast Rnt1p is required for cleavage of the pre-ribosomal RNA in the 39 ETS but not the 59 ETS.

LaCava, J., Houseley, J., Saveanu, C., Petfalski, E., Thompson, E., Jacquier, A., and Tollervey, D. (2005). RNA Degradation by the Exosome Is Promoted by a Nuclear Polyadenylation Complex. Cell *121*, 713–724.

Lemay, J.F., and Bachand, F. (2015). Fail-safe transcription termination: Because one is never enough. RNA Biol. *12*, 927–932.

Liu, J.-J., Niu, C.-Y., Wu, Y., Tan, D., Wang, Y., Ye, M.-D., Liu, Y., Zhao, W., Zhou, K., Liu, Q.-S., et al. (2016). CryoEM structure of yeast cytoplasmic exosome complex. Cell Res. *26*, 822–837.

Liu, Q., Greimann, J.C., and Lima, C.D. (2006). Reconstitution, Activities, and Structure of the Eukaryotic RNA Exosome. Cell *127*, 1223–1237.

Lykke-Andersen, S., Brodersen, D.E., and Jensen, T.H. (2009). Origins and activities of the eukaryotic exosome. J. Cell Sci. *122*, 1487–1494.

Mata, J., Marguerat, S., and Bähler, J. (2005). Post-transcriptional control of gene expression: a genome-wide perspective. Trends Biochem. Sci. *30*, 506–514.

Meng, W., and Nicholson, A.W. (2008). Heterodimer-based analysis of subunit and domain contributions to double-stranded RNA processing by Escherichia coli RNase III in vitro. Biochem. J. *410*, 39–48.

Mitchell, P., Petfalski, E., and Tollervey, D. (1996). The 3’ end of yeast 5.8S rRNA is generated by an exonuclease processing mechanism. Genes Dev. *10*, 502–513.

Mitchell, P., Petfalski, E., Shevchenko, A., Mann, M., and Tollervey, D. (1997). The Exosome: A Conserved Eukaryotic RNA Processing Complex Containing Multiple 3′→5′ Exoribonucleases.

Cell *91*, 457–466.

Moraes, K.C.M. (2010). RNA surveillance: molecular approaches in transcript quality control and their implications in clinical diseases. Mol. Med. *16*, 53–68.

Morton, D.J., Kuiper, E.G., Jones, S.K., Leung, S.W., Corbett, A.H., and Fasken, M.B. (2018). The RNA exosome and RNA exosome-linked disease. RNA *24*, 127–142.

Mühlemann, O., and Jensen, T.H. (2012). mRNP quality control goes regulatory. Trends Genet. *28*, 70–77.

Paul, B., and Montpetit, B. (2016). Altered RNA processing and export lead to retention of mRNAs near transcription sites and nuclear pore complexes or within the nucleolus. Mol. Biol. Cell *27*, 2742–2756.

Rondón, A.G., Mischo, H.E., Kawauchi, J., and Proudfoot, N.J. (2009). Fail-safe transcriptional termination for protein-coding genes in S. cerevisiae. Mol. Cell *36*, 88–98.

Roy, K., and Chanfreau, G. (2014). Stress-induced nuclear RNA degradation pathways regulate yeast bromodomain factor 2 to promote cell survival. PLoS Genet. *10*, e1004661.

Saavedra, C., Tung, K.S., Amberg, D.C., Hopper, A.K., and Cole, C.N. (1996). Regulation of mRNA export in response to stress in Saccharomyces cerevisiae. *10*.

Saavedra, C.A., Hammell, C.M., Heath, C. V., and Cole, C.N. (1997). Yeast heat shock mRNAs are exported through a distinct pathway defined by Rip1p. Genes Dev. *11*, 2845–2856.

Schneider, C., and Tollervey, D. (2013). Threading the barrel of the RNA exosome. Trends Biochem. Sci. *38*, 485–493.

Schuch, B., Feigenbutz, M., Makino, D.L., Falk, S., Basquin, C., Mitchell, P., and Conti, E. (2014). The exosome-binding factors Rrp6 and Rrp47 form a composite surface for recruiting the Mtr4 helicase. EMBO J. *33*, 2829–2846.

Singer-Krüger, B., and Jansen, R.P. (2014). Here, there, everywhere: mRNA localization in budding yeast. RNA Biol. *11*, 1031–1039.

Staals, R.H.J., and Pruijn, G.J.M. (2010). The Human Exosome and Disease. (Springer, New

York, NY), pp. 132–142.

Thoms, M., Thomson, E., Baßler, J., Gnädig, M., Griesel, S., and Hurt, E. (2015). The Exosome Is Recruited to RNA Substrates through Specific Adaptor Proteins. Cell *162*, 1029–1038.

Tudek, A., Porrua, O., Kabzinski, T., Lidschreiber, M., Kubicek, K., Fortova, A., Lacroute, F., Vanacova, S., Cramer, P., Stefl, R., et al. (2014). Molecular basis for coordinating transcription termination with noncoding RNA degradation. Mol. Cell *55*, 467–481.

Volanakis, A., Passoni, M., Hector, R.D., Shah, S., Kilchert, C., Granneman, S., and Vasiljeva, L. (2013). Spliceosome-mediated decay (SMD) regulates expression of nonintronic genes in budding yeast. Genes Dev. *27*, 2025–2038.

Wan, J., Yourshaw, M., Mamsa, H., Rudnik-Schöneborn, S., Menezes, M.P., Hong, J.E., Leong, D.W., Senderek, J., Salman, M.S., Chitayat, D., et al. (2012). Mutations in the RNA exosome component gene EXOSC3 cause pontocerebellar hypoplasia and spinal motor neuron degeneration. Nat. Genet. *44*, 704–708.

Wang, S.-W., Stevenson, A.L., Kearsey, S.E., Watt, S., and Bahler, J. (2008). Global Role for Polyadenylation-Assisted Nuclear RNA Degradation in Posttranscriptional Gene Silencing. Mol. Cell. Biol. *28*, 656–665.

Wasmuth, E. V., Januszyk, K., and Lima, C.D. (2014). Structure of an Rrp6–RNA exosome complex bound to poly(A) RNA. Nature *511*, 435–439.

Zinder, J.C., and Lima, C.D. (2017). Targeting RNA for processing or destruction by the eukaryotic RNA exosome and its cofactors. Genes Dev. *31*, 88–100.

Chapter 2

# Rrp6 cooperates with Slt2/Mpk1 and Paf1 independently of the RNA exosome to promote proper gene expression during heat stress

# Rrp6 cooperates with Slt2/Mpk1 and Paf1 independently of the RNA exosome to promote proper gene expression during heat stress

Charles Wang[1], Yanru Liu[1], Samuel M. DeMario[1], Igor Mandric[2], Carlos Gonzalez-Figueroa[1] and Guillaume F. Chanfreau[1,3*]

1. Department of Chemistry and Biochemistry, UCLA, Los Angeles, CA 90095, United States of America

2. Department of Computer Science, UCLA, Los Angeles, CA 90095, United States of America

3. Molecular Biology Institute, UCLA, Los Angeles, CA 90095, United States of America

*Corresponding Author

Email: guillom@chem.ucla.edu

**Summary**

The nuclear RNA exosome is a protein complex that is essential for RNA processing and degradation. Here we show that the nuclear-specific component of the exosome Rrp6p promotes cell survival during heat stress through the cell wall integrity (CWI) pathway, independently of its catalytic activity or association with the core exosome. Rrp6p exhibits negative genetic interactions with the Mpk1p or Paf1p elongation factors required for expression of CWI genes during stress. Overexpression of Rrp6p, its catalytically inactive or exosome-independent mutant can partially rescue the growth defect of the *mpk1Δ* mutant and stimulates expression of the Mpk1p target gene *FKS2*. The *rrp6Δ* and *mpk1Δ* mutants show similarities in deficient expression of cell wall genes during heat shock, and overexpression of a single CWI gene *HSP150* gene can rescue the heat-induced lethality of the *mpk1Δrp6Δ* mutant. These results demonstrate that Rrp6p moonlights independently from the exosome to synergize the functions of Mpk1p and Paf1p in ensuring proper expression of CWI genes and cell survival during heat stress.

**Keywords**

*RRP6*, *MPK1*, *PAF1*, cell wall stress, cell wall integrity pathway, heat stress response, gene expression, gene regulation, RNA processing.

## Introduction

The nuclear exosome complex plays a diverse role in RNA metabolism, from RNA processing to the surveillance and degradation of defective RNAs (Zinder and Lima, 2017). The nuclear exosome contains ribonuclease activities that are essential for the proper 3´ end trimming and maturation of RNAs including small nuclear RNAs (snRNAs), small nucleolar RNAs (snoRNAs) and ribosomal RNAs (rRNAs) (Allmang et al., 1999; Bernstein and Toth, 2012). Furthermore, the surveillance and degradation of improperly processed RNAs limits the export and translation of faulty RNAs that may otherwise be detrimental (Moraes, 2010). The nuclear exosome function is also coupled to regulatory pathways for the proper control of gene expression (Bresson et al., 2017; Volanakis et al., 2013). Mutations within genes encoding exosome subunits are responsible for several human diseases, including neurological disorders and cancers—underscoring the importance of functional exosome activity for cellular homeostasis and proper human development (Fasken et al., 2017; Gillespie et al., 2017; Morton et al., 2018; Wan et al., 2012).

In *S. cerevisiae*, the core ring of the nuclear exosome consists of a family of 6 RNase PH homologs and 3 RNA binding proteins (Bernstein and Toth, 2012; Sloan et al., 2012; Zinder and Lima, 2017). This core contains no exoribonuclease activity and instead relies on two associated proteins for its degradative functions; Dis3p/Rrp44p is a processive exoribonuclease with additional endonuclease activity, while Rrp6p has distributive exonucleolytic activity (Bernstein and Toth, 2012; Sloan et al., 2012). The absence of Rrp6p is viable in *S. cerevisiae* and deletion of the *RRP6* gene has been broadly used as a method to partially inactivate the nuclear exosome. The deletion of *RRP6* results in a slow growth phenotype in addition to the accumulation of many noncoding RNAs, RNA degradation intermediates and unprocessed or extended 3´ end RNAs (Burkard and Butler, 2000; Butler and Mitchell, 2010; Feigenbutz et al., 2013a; Fox and Mosley, 2016). Although Rrp6p works in concert with the core exosome to process or degrade its RNA substrates (Wasmuth and Lima, 2017), several studies have

suggested an exosome-independent function of Rrp6p (Callahan and Butler, 2008; Fox et al., 2015; Graham et al., 2009). The ability of Rrp6p to function outside of the nuclear exosome raises the possibility of other Rrp6p dependent processes or complexes that may be important under specific growth conditions, including stress.

During stress, specific transcription factors are activated to rapidly alter gene expression and maintain homeostasis to promote cell survival. The mitogen-activated protein kinase (MAPK) cascade is an evolutionarily conserved pathway that regulates these transcription factors during adverse environmental stresses (Gustin et al., 1998; Hahn and Thiele, 2002; Kim et al., 2010; Levin, 2005). Mpk1p (also known as Slt2p) is a kinase involved in the cell wall integrity (CWI) pathway, a MAPK cascade involved in maintaining and monitoring the integrity of the cell wall in *S. cerevisiae* (Fig 1A; Kim and Levin, 2011). Once activated by upstream kinases, Mpk1p performs multiple functions to alter gene expression; it phosphorylates the transcription factors Rlm1p and Swi4p/Swi6p to stimulate their binding to DNA (Fig 1A), regulates transcription initiation and elongation directly through a non-catalytic mechanism involving the Paf1 complex (Fig 1A), and retains the bulk of mRNAs within the nucleus through an unknown mechanism (Carmody et al., 2010; Jin et al., 2014; Kim et al., 2010). Additionally, Mpk1p directly influences RNA polymerase II (RNAP II) activity by phosphorylating the Tyr1 residues of the YSPTSPS repeats of the C-terminal domain (CTD) of the large subunit of RNAP II (Yurko et al., 2017). Altogether, these multiple roles of Mpk1p along with associated CWI factors result in a remodeling of the cell wall composition and an overall increase in the thermotolerance of the cell (Brul et al., 2000). Perturbation of the activity of CWI factors result in the down-regulation of a subset of cell wall proteins and consequently a decrease in the ability of cells to handle their internal turgor pressure (Brul et al., 2000; Levin, 2005). This results in a osmoremedial lethal phenotype at high temperatures (Brul et al., 2000; Levin, 2005).

In this study we provide genetic evidence for a novel role of Rrp6p in promoting cell survival during heat stress through the CWI pathway, and we show that Rrp6p contributes to proper

gene expression during stress in a manner similar to Mpk1p. The role that Rrp6p plays in this pathway is independent of its RNase activity and of its association with the nuclear exosome. Together, our data identify a unique exosome-independent function for Rrp6p in synergizing the roles of the Mpk1p and Paf1p elongation factors in the proper induction of the CWI gene expression program during stress.

## Results

### Rrp6p plays a critical role in the heat stress response pathway of *S. cerevisiae*

*S. cerevisiae* strains lacking Rrp6p are viable, but loss of Rrp6p results in a temperature sensitive phenotype (ts) (Fig 1B). Although this ts phenotype could be due to a destabilization of the core exosome at higher temperatures in the absence of Rrp6p, it could also indicate that Rrp6p plays an exosome-independent role in promoting fitness during cellular stress. To further investigate this potential role, we deleted Rrp6p in conjunction with the mitogen-activated protein kinase (MAPK) Slt2p, also known as Mpk1p. The absence of Mpk1p compromises the CWI pathway and sensitizes yeast cells to specific cell wall stresses, including growth at higher temperatures (Brul et al., 2000). Strikingly, the *mpk1Δrrp6Δ* double mutant was not viable at 37°C, a much more severe phenotype compared to the slow growth of the individual mutants at the same temperature (Fig 1B). As growth at 37°C induces cell wall stress, we hypothesized that the synthetic lethality was the result of a weakened cell wall with an inability to tolerate differences in osmotic potential. If so, addition of an osmotic support would restore the growth of the double mutant. As predicted, the lethality of the *mpk1Δrrp6Δ* strain at 37°C was rescued by the addition of 1M sorbitol or 0.6M KCl (Fig 1C). This result indicates that lethality of the *mpk1Δrrp6Δ* strain at 37°C is a direct result of compromised cell wall integrity, potentially because of improper expression and biogenesis of cell wall proteins. Osmotic support had no additional effect on the growth of the *rrp6Δ* single mutant, suggesting that the potential role for Rrp6p in the CWI pathway is not the growth limiting factor for this mutant at 37°C.

We next asked whether the lethality of the *mpk1Δrrp6Δ* strain at higher temperatures was specific to the absence of the nuclear exonuclease Rrp6p or if the inactivation of cytoplasmic RNA processing or degradation factors may exhibit similar phenotypes. To answer this question, we deleted Mpk1p along with the cytoplasmic exoribonuclease Xrn1p, the nonsense mediated decay factor Upf1p or the cytoplasmic exosome factor Ski2p (Parker, 2012). These mutants were chosen to disable a variety of RNA processing and degradation processes. However, none of these double mutations phenocopied the temperature sensitivity of the *mpk1Δrrp6Δ* cells (Fig S1A). This suggests that the lethality of the *mpk1Δrrp6Δ* mutant is specific to the absence of the nuclear exosome protein Rrp6p, rather than being due to general defects in RNA metabolism. Together, these data demonstrate a negative genetic interaction between Rrp6p and Mpk1p during stress, suggesting that the two proteins may cooperate to maintain the integrity of the cell wall and promote cell survival under heat stress.

**The role of Rrp6p in the heat stress response pathway is independent of its catalytic activity or association with the core exosome**

The previous observations raised the question of how Rrp6p and Mpk1p cooperate to promote cell survival during growth at non-permissive temperatures. The nuclear RNA processing or degradation defects associated with the absence of Rrp6p may impede the rapid changes of mRNA abundance and gene expression that are necessary for adaption to environmental stresses. If the temperature sensitivity of *mpk1Δrrp6Δ* mutant were due to a general deficiency in nuclear exosome function at high temperatures, a similar lethal phenotype would be expected if the genetic deletion of Mpk1p is combined with other mutations that inhibit functions of the nuclear exosome. This can be achieved through the removal of the nuclear exosome cofactor Rrp47p, or through a point mutation within the core exosome protein Rrp40 (*Rrp40-W195R*) that prevents its stable association with the exosome complex and its nuclear cofactor Mpp6p (Butler and Mitchell, 2010; Fasken et al., 2017; Gillespie et al., 2017). Strikingly, both

*mpk1Δrrp47Δ* and *mpk1Δrrp40-W195R* mutant strains were viable when grown at high temperatures, and in fact grew better than the single *mpk1Δ* mutant alone (Fig 1D). A similar rescue in growth was observed in the *mpk1*Δ*mpp6*Δ mutant at 37°C as well (Fig S1B). These results suggest that the lethality of the *mpk1Δrrp6Δ* strain is not due to a general inactivation of the nuclear exosome, but rather because of an exosome-independent function of Rrp6p. The *rrp40-W195R* mutation or the loss of Mpp6p did not impact Rrp6p protein levels compared to WT at 37°C (Fig S2A), but a decrease of Rrp6p protein abundance was detected in the *rrp47*Δ mutant at 37°C (Fig S2A), consistent with a previous study (Feigenbutz et al., 2013b). Because these three strains did not impact Rrp6p protein levels in a consistent manner, we postulate that the fitness gain of the *mpk1Δrrp47Δ, mpk1Δrrp40-W195R* and *mpk1*Δ*mpp6*Δ strains at elevated temperatures compared to the single *mpk1Δ* mutant could be due to a relative increase in the free available pool of Rrp6p arising from the destabilizing effect of the absence of Rrp47p, Mpp6p or of the Rrp40p point mutations on Rrp6p association with the exosome. To further test this hypothesis, we deleted the chromatin remodeler Isw1p, which cooperates with Rrp6p to promote mRNA retention during stress (Babour et al., 2016). Indeed, Isw1p deletion also rescued the heat sensitivity of the *mpk1Δ* mutant (Fig 1D), consistent with the idea that dissociating Rrp6p from any of its associated factors (Isw1p or the nuclear exosome) can positively impact the CWI response. Finally, overexpression of Rrp6p independently from any other exosome component improved the growth of the *mpk1Δ* mutant at 37°C (Fig 1E and 2D). This result demonstrates that the core exosome is not required to mediate the role that Rrp6p plays in promoting cell survival during stress.

To further explore the hypothesis of an exosome-independent function of Rrp6p in the stress response pathway, we expressed a mutant form of Rrp6 (*rrp6-C2Δ*) (Fig 2A) that cannot associate with the nuclear exosome (Callahan and Butler, 2008), and tested its ability to promote the growth of the *mpk1Δ* mutant at 37°C. Strikingly, overexpression of *rrp6-C2*Δ improved the growth of the *mpk1*Δ mutant under heat stress (Fig 2D), confirming our notion of

an exosome-independent function of Rrp6p. We next determined whether the expression of *rrp6-C2*Δ may rescue the growth lethality of the *mpk1*Δ*rrp6*Δ mutant at high temperatures. Because strains were grown on minimal media for plasmid selection, the lethality of the *mpk1Δrrp6Δ* strain was detected at a lower temperature (35°C). Remarkably, expression of the *rrp6-C2Δ* mutant rescued the growth of the *mpk1Δrrp6Δ* mutant at 35°C and promoted a growth rate similar to that of the *mpk1Δ* mutant harboring an empty vector (Fig 2B). This effect was not due to differences in protein stability as no detectable differences in protein abundance were observed between the exogenously expressed wild type Rrp6p and the C2Δ mutant before and after heat stress (Fig S2B). This result provides further support for the conclusion that Rrp6p plays a role in the CWI pathway independently from its involvement with the nuclear exosome.

A role for Rrp6p in promoting cellular survival independently from the nuclear exosome may or may not require its exonuclease catalytic activity. We expressed a catalytically inactive version of Rrp6p (*rrp6-D238N)* (Fig 2A) to determine if Rrp6p catalytic activity was necessary to improve the growth of the *mpk1Δ* mutant at 37°C. The *rrp6-D238N* mutant is void of all exonuclease activity (Callahan and Butler, 2008) and does not improve the slow growth phenotype of the *rrp6Δ* mutant under heat stress when expressed exogenously (Fig 2C). Nonetheless, expression of the *rrp6-D238N* mutant improved the growth of the *mpk1*Δ mutant at 37°C (Fig 2D). In fact, expression of either *rrp6-D238N* or *rrp6-C2*Δ mutants rescued the growth of the *mpk1*Δ mutant more so than the expression of wild-type *RRP6* (Fig 2D). These data suggest that these Rrp6p mutants may be better catered to fulfilling its stress response functions without the restraint of its exosome or exonuclease functions. Furthermore, the catalytically inactive Rrp6p mutant rescued the growth of the *mpk1Δrrp6Δ* strain at high temperature, showing that the function of Rrp6p in the stress response pathway is indeed independent of its exonuclease activity (Fig 2C). The catalytically inactive Rrp6p was expressed at levels comparable to wild type before and after heat stress (Fig S2B). To ascertain the absence of any exonuclease activity that may contribute to the rescue of growth, northern blot analysis was performed with

probes corresponding to the ITS2 region of the rRNA, a *bona fide* substrate of the nuclear exosome (Callahan and Butler, 2008). As expected, an increase in the 7S rRNA processing intermediate was detected in the *rrp6Δ* and *mpk1Δrrp6Δ* mutants carrying an empty vector, as these mutants lack Rrp6p to properly process this intermediate (Fig S2E, lanes 5 and 7). Similarly, an accumulation of the 7S was detected when the catalytically inactive Rrp6p mutant was exogenously expressed in the *rrp6Δ* and *mpk1Δrrp6Δ* mutant strains, confirming that *rrp6-D238N* is indeed catalytically inactive (Fig S2E, lanes 6 and 8). Moreover, expressing the *rrp6-D238N* mutant negatively impacts rRNA processing, as shown by a higher accumulation of the 7S rRNA intermediate in these strains compared to the *rrp6Δ* and *mpk1Δrrp6Δ* mutants alone. We speculate that the catalytically inactive *rrp6-D238N* mutant may further inhibit 7S processing by binding to and stabilizing this rRNA intermediate and preventing further trimming by the core exosome. Thus, despite exacerbating rRNA processing defects, a catalytically inactive *rrp6-D238N* mutant could still promote survival of the *mpk1Δrrp6Δ* strain in stress conditions, further strengthening the idea that Rrp6p functions independently from the exosome during stress.

To further assess the protein domains of Rrp6p involved in its stress-related functions along Mpk1p, we used a C-terminally TAP-tagged version (Fig 2A), which we originally thought of using for proteomics studies. Strikingly, the Rrp6p-TAP strain was unviable at 37°C (Fig 2E). This phenotype is not due to thermal instability of the TAP-tagged version of Rrp6p as it is expressed at levels similar to wild-type at all temperatures (Fig S2C). Despite normal expression, the TAP-tagged version of Rrp6p is clearly defective for exosome function, as shown by an accumulation of 7S intermediates similar to that of the *rrp6Δ* strain at all temperatures (Fig S2F). This result could be due to the role of the C-terminus of Rrp6p in promoting exosome activation (Wasmuth and Lima, 2017), which may be compromised by the addition of a TAP-tag at the C-terminus. However, unlike the *rrp6Δ* strain, the growth phenotype of the Rrp6-TAP strain at elevated temperatures could be rescued by adding sorbitol

(Fig 2E), showing that the lethality of the TAP-tagged strain at 37°C is not due to inactivation of the exosome, but rather because of the inability of the TAP-tagged version of Rrp6p to function in the CWI pathway. Altogether, these data demonstrate that delayed or defective RNA processing is not responsible for the lethality of the *mpk1Δrrp6Δ* mutant at high temperatures, and that the involvement of Rrp6p in the stress response is independent of its exonuclease activity or association with the nuclear exosome.

**Rrp6p function in the CWI pathway requires the interaction between Mpk1p and Paf1p**

We next sought to explore the role that Rrp6p plays in the CWI pathway. To this end, we created several mutants in which Rrp6p is deleted along with other CWI factors depicted in Fig 1A. These included the pseudokinase Kdx1p, the downstream transcription factor Swi4p, and the RNA polymerase II-associated elongation factor Paf1p which functions downstream of Mpk1p (Levin, 2005). The *kdx1Δrrp6Δ, swi4Δrrp6Δ* and *paf1Δrrp6Δ* mutant strains were monitored for growth at 30°C or 37°C. There was no detectable growth defect associated with the *swi4Δrrp6Δ* or *kdx1*∆*rrp6*∆ mutants at 37°C (Fig S3A). However, similarly to the *mpk1Δrrp6Δ* mutant, the *paf1Δrrp6Δ* mutant was not viable at high temperatures (Fig 3A), strengthening the connection between Rrp6p and the branch of the CWI pathway regulated by Mpk1p and Paf1p (Fig 1A).

Further experiments showed that the phenotype of the *paf1Δrrp6Δ* mutant mirrors that of the *mpk1Δrrp6Δ* mutant. The lethality of the *paf1Δrrp6Δ* mutant at high temperature could be rescued through the addition of osmotic support (Fig 3A), or by expressing the exosome independent mutant *rrp6-C2Δ* (Fig S3B). As Paf1p is involved in all aspects of RNA Pol II transcription cycle (Van Oss et al., 2017), its absence may attenuate multiple processes in addition to CWI. This may explain the difficulty of the *rrp6-C2Δ* mutant in rescuing the growth lethality of the *paf1Δrrp6Δ* mutant at 35°C, and the complete inability of the *rrp6-D238N* mutant to do so. Nonetheless, these results indicate that Rrp6p function in the CWI pathway involves

Mpk1p and the downstream RNA polymerase associated factor Paf1p. As Paf1p resides within the Paf1 complex (Paf1C), we tested if the deletion of Rrp6p along with other Paf1C associated factors, such as Leo1p and Rtf1p would exhibit a similar growth defect under heat stress. The absence of both Rtf1p and Rrp6p did not have any major impact on growth at 30°C and at 37°C (Fig 3B). However, co-deletion of Rrp6p and Leo1p resulted in a severe slow growth phenotype compared to the single mutants alone (Fig 3B). This result confirms the genetic interaction between Rrp6p and the Paf1 complex and suggests a possible molecular basis for the lethality of *mpk1Δrrp6Δ* at 37°C. The absence of Leo1p may not impact the function of the Paf1 complex to the same extent as deleting Paf1p, which may explain why the *leo1*Δ*rrp6*Δ mutant was not lethal at 37°C. This is consistent with the observation that only the single *paf1Δ* mutant displays a slow growth phenotype when compared to *leo1Δ* and *rtf1Δ* alone (Fig 3B) and with previous studies showing that Paf1p is critical for the stability of the Paf1 complex (Van Oss et al., 2017).

To demonstrate that the role of Rrp6p in the CWI pathway requires the interaction of Mpk1p with Paf1p, we used strains expressing a catalytically inactive version of Mpk1p (*mpk1-K54R*) void of its kinase activity, or a non-phosphorylatable mutant form (*mpk1-TAYF*). The *mpk1-TAYF* mutant cannot be phosphorylated by upstream factors, which prevents it from associating with Paf1p (Kim and Levin, 2011). If the interaction between Mpk1p and Paf1p is critical to Rrp6p role in the CWI pathway, this *mpk1-TAYF* mutant should be unable to rescue the growth of the *mpk1Δrrp6Δ* mutant under heat stress. By contrast, the catalytically inactive *mpk1-K54R* mutant can interact with Paf1p but is incapable of phosphorylating other downstream factors. Strikingly, expression of *mpk1-TAYF* did not rescue the growth of the *mpk1Δrrp6Δ* strain at 35°C (only suppressor colonies were observed). However, growth rescue was detected when expressing the *mpk1-K54R* mutant (Fig 3C). The differences in growth rates between the different versions of Mpk1p were not due to differences in protein stability, as the two mutant versions were expressed to levels similar or slightly lower to those of wild-type Mpk1p (Fig S2D). Overall these data show that the lethality of the *mpk1Δrrp6Δ* strain in stress conditions is due to the inability of

Mpk1p to interact with the downstream factor Paf1p to regulate gene expression, and not due to the loss of its kinase activities. They also show that Rrp6p is involved in promoting heat stress response in a specific branch of the CWI pathway (Fig 1A) that requires the Mpk1•Paf1 complex independently from the kinase activity of Mpk1p.

**Rrp6p cooperates with Mpk1p for proper gene expression during heat stress**

Mpk1p and kdx1p promote transcriptional elongation of stress responsive genes, such as *FKS2*, through a physical interaction with Paf1p (Kim and Levin, 2011). To determine whether Rrp6p may play a role in this process, we overexpressed Rrp6p in WT and *mpk1Δkdx1*Δ strains, and analyzed its effect on *FKS2* expression during heat shock. Strikingly, Rrp6p overexpression increased the transcript levels of *FKS2* in both strains (Fig 4A), suggesting a role for Rrp6p in promoting expression of this stress-induced gene. By contrast, the overexpression of Rrp6p did not increase the transcript abundance of *RPS12,* which we show below is repressed before and after heat shock in the *mpk1Δkdx1*Δ mutant (Fig 4A). This suggests that the overexpression of Rrp6p does not stabilize RNA transcripts on a global scale through altering exosome activity. The overexpression of *rrp6-C2*Δ and *rrp6-D238N* in WT and the *mpk1Δkdx1*Δ mutant both increased the transcript abundance of *FKS2* in these strains post heat shock as well (Fig 4B). This result supports our previous observation that the overexpression of *RRP6, rrp6-C2*Δ and *rrp6-D238N* all promote the growth of the *mpk1*Δ mutant at 37°C (Fig 2D). Because the Rrp6p-C2Δ does not associate with the nuclear exosome, its overexpression is not expected to impact exosome function. These results identify a role for Rrp6p in the expression of CWI target genes and suggest that the lethality of the *mpk1Δrrp6Δ* strain at 37°C is due to changes in gene expression that result in a defective cell wall. This observation led us to perform RNA-seq analysis of the *mpk1Δrrp6Δ* mutant and of control single mutant and WT strains before, and after a 45-minute heat shock at 42°C. Although this heat shock condition is different from the

temperatures used previously for growth at steady state, it was chosen to detect rapid responses to heat stress at the RNA level without attenuation due to longer exposures.

RNA-seq analysis revealed the repression of a large number of genes in the *mpk1Δ*, *rrp6Δ* and *mpk1Δrrp6Δ* mutant strains compared to wild-type in heat shock conditions (Fig 5A). By contrast, the number of genes down-regulated compared to the wild-type before heat shock was much lower in all of these mutants (Fig 5A, upper Venn Diagram). Most notably, the large majority of genes repressed in heat shock compared to the wild-type is shared between the *mpk1Δ* and *rrp6Δ* mutant strains (Fig 5A), which further support a shared biological function between these two proteins. Importantly, this overlap is much less pronounced for RNAs repressed in these mutants prior to heat shock, further strengthening the unique role of Rrp6p along with Mpk1p during heat shock. The full list of genes up- or down-regulated in each of the mutants is presented in Table S1. GO analysis of repressed genes shared between the *mpk1Δ* and *rrp6Δ* mutant strains in heat shock conditions showed an enrichment for cell wall proteins, protein transporters and ribosomal protein genes (RPGs) (Table S1). However, we do not think that the decrease in RPG expression is due to a direct role for Rrp6p in their expression, as Rrp6p overexpression could not rescue the downregulation of *RPS12* detected in the *mpk1Δ* mutant (Fig 4A). Focusing on cell wall genes revealed a large decrease in the expression of the *HSP150* gene in the *mpk1Δrrp6Δ* mutant under heat shock. This decrease in *HSP150* expression may play a significant role in the cellular phenotype of the double mutant, as *HSP150* encodes a cell wall protein necessary for cell wall stability (Russo et al., 1992). Although we were unable to detect an increase in *HSP150* expression in our heat shock conditions, the decreased expression in the *mpk1Δrrp6Δ* mutant was confirmed by northern blot analysis (Fig 5B). The decrease in *HSP150* expression was not due to a general defect in the expression of heat shock protein genes as *HSP12* was still robustly induced in the *mpk1Δrrp6Δ* mutant (Fig 5B). Consistent with a role for Rrp6p in promoting *HSP150* expression during heat

shock, overexpression of *RRP6, rrp6-C2*Δ and *rrp6-D238N* slightly increased *HSP150* transcript abundance in the *mpk1*Δ*kdx1*Δ mutant post heat shock (Fig 4B).

### *HSP150* overexpression promotes survival of the *mpk1Δrrp6Δ* mutant in heat stress

Based on the previous observations, we hypothesized that a defect in *HSP150* expression may be a contributing factor in the inability of the *mpk1Δrrp6Δ* strain to survive under heat stress. To test this hypothesis, we constructed an *HSP150* overexpression plasmid based on the yeast multicopy vector YEp24, which overexpresses *HSP150* from a *TEF*1 promoter. The use of this promoter alleviates any potential decrease in *HSP150* expression that might be dependent on its endogenous promoter and its association with stress-specific transcription factors. Strikingly, *HSP150* overexpression promoted survival of the *mpk1Δrrp6Δ* mutant under heat stress (Fig 5C). Importantly, the overexpression of *HSP150* did not rescue the growth of another severely heat sensitive mutant strain lacking the RNase III endonuclease Rnt1p (Fig 5D) at the same temperature. This result shows that the rescue with *HSP150* overexpression is specific to *mpk1Δrrp6Δ* cells in which its expression is deficient. We note that *HSP150* overexpression does not fully rescue the growth of the *mpk1Δrrp6Δ* mutant, as it is highly likely that other improperly expressed genes may also contribute to the lethality of the *mpk1Δrrp6Δ* mutant strain at elevated temperatures, despite *HSP150* being a major contributor. Taken together, these results shown that Rrp6p along with Mpk1p and possibly Paf1p are required to ensure proper expression of *HSP150*, and potentially other CWI genes, to promote cell survival during stress.

How Mpk1p, Paf1p and Rrp6p cooperate to ensure proper gene expression during heat stress remains unknown. We were unable to detect a stable interaction between Rrp6p and Mpk1p based on co-immunoprecipitation experiments (Fig S4A). Since the role of Rrp6p in stress is independent from its exonuclease activity, we hypothesized that the stress-induced expression of RNAs stemming from the CWI pathway requires Rrp6p for proper transcription. This led us to

investigate if Rrp6p may alter RNAP II phosphorylation state. Mpk1p has been shown to phosphorylate the Tyr1 residues of the CTD of RNAP II during multiple stress responses and impact gene expression (Yurko et al., 2017). However, no differences in Tyr1 phosphorylation was observed for RNAPII CTD in our mutant strains under heat stress (Fig S4B). Further studies are required to precisely identify the role Rrp6p plays with Mpk1p and Paf1p to promote cell survival during stress.

**Discussion**

In this study, we demonstrated an undiscovered yet critical role of Rrp6p in promoting cellular survival during heat stress. This role is remarkably independent of both its catalytic activity and association with the nuclear exosome. This unique function of Rrp6p includes but may not be limited to its ability to synergize the roles of the Mpk1p and Paf1p components of the CWI pathway to promote proper expression of CWI genes and strengthen the cell wall. Although further biochemical work is necessary to characterize the precise mechanism behind this unique function of Rrp6p, our results show that it may be linked to the necessity of expressing specific mRNAs during stress. Strikingly, restoring the expression of a single target gene, *HSP150,* was sufficient to rescue the growth of the *mpk1Δrrp6Δ* mutant at high temperatures. This result, along with the osmoremedial phenotype of this mutant, provide major evidence for the fact that defective induction of CWI genes caused by simultaneous inactivation of Mpk1 and Rrp6p is the direct cause of cellular lethality. However, it is likely that defective expression of a diverse subset of genes in the absence of Rrp6p may partially contribute to the overall decrease of cellular fitness in this background as well.

Interestingly, the exosome had previously been linked to heat-shock related gene expression, as previous work in *Drosophila* had shown that the exosome associates with heat shock genes during stress (Andrulis et al., 2002). However, the data presented here demonstrate that the

role of Rrp6p is independent of the core exosome, which suggests that the mechanisms involving the exosome in stress-related gene expression may have diverged during evolution. Rrp6p has also been shown to function along Isw1p in mRNP retention at the site of transcription during heat shock (Babour et al., 2016). However, we show that the genetic inactivation of Rrp6p and Isw1p have opposite effects when combined with Mpk1p inactivation (Fig 1D), which shows that the role of Rrp6p in the CWI pathway is not linked to its function in mRNP retention during stress. The role of Rrp6p in the CWI pathway is clearly independent from its association with the exosome, as demonstrated by the results obtained with the C2Δ mutant, with mutants that impact other exosome subunits, or by overexpressing Rrp6p and its mutants, all of which have a positive effect on cell survival through the CWI pathway (Fig 1D and E, Fig 2B-D). Therefore, Rrp6p must somehow exist in the cell as free pool during stress, perhaps as a result of increased synthesis, or by dissociating from the exosome. We did not detect any increase of Rrp6p expression during heat shock by Western blot (Fig S2B and C, Fig S4A), which seems to eliminate the former hypothesis. Thus, it is possible that a subpopulation of Rrp6p may dissociate from the core exosome during stress such that Rrp6p may fulfill its function in CWI. Alternatively, it is possible that Rrp6p proteins newly synthesized after heat shock may not associate with other exosome subunits, but instead function independently and possibly associate with the chromatin to promote proper transcriptional elongation along with Mpk1p and Paf1p. Such association with the chromatin to modulate transcriptional complexes would not be unexpected as Rrp6p has been shown to mediate transcriptional termination (Fox et al., 2015).

Altogether, this study demonstrates a unique and specialized function of Rrp6p in promoting gene expression independently of the core exosome and of its ribonucleolytic activity. Although this novel function operates in the context of the CWI pathway, it is possible that Rrp6p may also function in other biological processes under various cellular growth conditions. The full

extent of Rrp6p influence on RNA metabolism remains to be explored and may provide further evidence on the substantial functional complexity of this protein in cellular physiology.

**Acknowledgements**

We thank David E. Levin and Christopher D. Lima for their generous gift of the Mpk1 mutant plasmids and the α-RRP6 antibodies, respectively, Indya Weathers for her dedication and extensive technical assistance and Yerbol Kurmangaliyev for his assistance in demultiplexing our RNA-seq data. This work was supported by the National Institute of General Medical Sciences Grant R35 GM130370. C.W. was supported by the National Research Service Award Training Grant GM007185.

**Author Contributions**

Conceptualization and Methodology, GC and CW; Investigation, CW, CG and YL; Bioinformatics, SD and IM; Writing – Original Draft, CW; Writing – Review and Editing, GC; Funding Acquisition, GC.

**Declaration of Interest**

The authors declare no competing interests.

**Figure Legends**

**Figure 1. Genetic interaction between Mpk1p, Rrp6p and Nuclear exosome or Rrp6-associated proteins.**

(A) The cell wall integrity (CWI) pathway. Adapted from (Kanehisa and Goto, 2000).

(B) Genetic interactions between Mpk1p and Rrp6p.

(C) The negative genetic interaction between the *mpk1Δ* and *rrp6Δ* mutants can be rescued by osmotic support.

(D) Deletion or mutation of Rrp6-associated proteins (Rrp40p, Rrp47p, Isw1p) rescues the ts phenotype of the *mpk1Δ* mutant strain.

(E) Overexpression of Rrp6p partially rescues the heat sensitivity of the *mpk1Δ* mutant.

For panels B-E, 5-fold serial dilutions of indicated strains were spotted onto the respective plates. Plates were grown at 30°C, 35°C or 37°C for the indicated number of days.

**Figure 2. Contribution of Rrp6p structural domains to cell survival in stress conditions.**

(A) Schematic diagram of Rrp6p and its various mutants. The TAP tag consists of a calmodulin binding peptide followed by a TEV protease cleavage site and two protein A domains. Domain structure of Rrp6p is adapted from (Wasmuth and Lima, 2017).

(B-E) 5-fold serial dilution of the strains expressing the versions of Rrp6p shown in (A) were spotted onto YPD or SD-URA plates and grown for the indicated number of days at the indicated temperatures.

**Figure 3. Rrp6p function in the heat stress response pathway requires Paf1p and its interaction with an activated Mpk1p.**

(A-C) 5-fold serial dilution of the indicated strains grown at the indicated temperature and growth medium. Plates were grown for the indicated number of days.

**Figure 4. Rrp6p is required for proper expression of CWI genes along with Mpk1p.**

(A-B) Representative northern blot analysis of the *FKS2, RPS12* and *HSP150* mRNAs in the indicated strains and conditions. scR1 or *TDH1* was used as a loading control. A minimum of three biological replicates were performed and the quantification and standard error are shown.

**Figure 5. The cell wall protein Hsp150p is not expressed properly in the *mpk1Δrrp6Δ* mutant and can rescue the heat sensitivity of this mutant.**

(A) Venn diagram of down-regulated genes between the *mpk1Δ, rrp6Δ,* and *mpk1Δrrp6Δ* mutants compared to WT before (25°C) and after a 45 minutes heat shock at 42°C.

(B) Northern blot analysis of *HSP150* expression in the indicated strains.

(C-D) 5-fold serial dilution of the indicated strains grown on SD-URA plates at 30°C or 35°C. Plates were incubated for the indicated number of days.

## STAR Methods

### Experimental model and subject details

### Strain construction

Unless otherwise noted, all strains used in this study were either obtained from the GE Dharmacon Yeast Knockout collection or derived from BY4742 and listed in Supplemental Material (Table S2). Mutant strains were constructed using the lithium acetate/PEG/Single stranded carrier DNA transformation method (Gietz and Schiestl, 2007) with PCR products containing flanking regions of the area of interest for homologous recombination. The PCR products used in these transformations were produced from template plasmids as described in (Longtine et al., 1998). Transformants are grown on plates supplemented with antibiotics and/or on drop out plates before being streaked for single colonies. Successful transformants are

confirmed through the extraction of its genomic DNA to be used for PCR using primers specific to the region of interest. Incorporation of plasmids into yeast was performed using the same lithium acetate/PEG/Single stranded carrier DNA transformation method mentioned above.

**Yeast culturing**

Yeast cultures were grown in either YPD (1% w/v yeast extract, 2% w/v peptone, and 2% w/v dextrose) or in appropriate drop out minimal media (0.67% w/v yeast nitrogen base, 2% w/v dextrose, and 0.2% w/v amino acid mixture). Unless otherwise described, 50ml cultures were grown at the standard 30°C to exponential phase ($OD_{600nm}$ of ~0.4-0.6) for spot dilution analysis or to be flash frozen in liquid nitrogen for downstream usage. For heat shock experiments, cells were grown at 23°C steady state to an $OD_{600nm}$ of ~0.4-0.6 before equal volumes of prewarmed media was added to acquire the desired final temperature.

**Cloning and bacterial transformations**

All PCRs done for cloning uses the high-fidelity polymerase Phusion Hi-Fi (New England Biolabs). Cloning of *RRP6* into YEp24 was done using standard procedures. Briefly, the *RRP6* template was PCR amplified with primers flanked by Sac1 or SphI restriction cut sites. The template was then cut by the respective restriction enzymes before being column purified (Biopioneer). The YEp24 vector was cut by the same restriction enzymes before being treated with CIP phosphatase (New England Biolabs) prior to column purification. Ligation of the insert and vector were done using a T4 DNA ligase (Life Technologies) before being transformed into competent DH5α E.coli cells. Transformed cells were plated on LB plates supplemented with ampicillin and positive clones were confirmed through colony PCR.

Cloning of *HSP150* with a *TEF1* promoter in YEp24 was done using a Quick-Fusion cloning kit (Bimake). Here, the *TEF1* promoter was PCR amplified using the pFA6a-FRB-KANMX as a template (Longtine et al., 1998). The amplified *TEF1* promoter product was designed to contain a BamHI cut site in its 5´end and overlapping regions with the *HSP150* template in its 3´end. The *HSP150* template was amplified from yeast genomic DNA. This *HSP150* template was

designed to contain a homology region to the *TEF1* promoter template on its 5´end and a SphI restriction cut site on its 3´end. These PCR products along with a linearized YEp24 vector were used in the Quick-Fusion Cloning reaction according to manufacturer protocol. All oligonucleotides used are found in Supplemental Table S4

**Plasmid site directed mutagenesis**

The YEp24 plasmids containing the mutant forms of *RRP6* were created through site-directed mutagenesis using the QuikChange Lightning Site-Directed Mutagnesis Kit (Agilent Technologies) according to manufacturer protocol. The oligonucleotides used were designed by the online QuikChange Primer Design tool and can be found in the Supplemental Table S4

**Yeast spot dilutions**

Yeast cultures were grown to an exponential phase of $OD_{600nm}$ of ~0.4-0.6 in appropriate media. Within a 96 well plate, each culture was then diluted to an $OD_{600nm}$ of 0.05 in 100uL of media. Serial dilutions were performed 5 times, where each time a 30uL of cell suspension was added to 100uL of media. 5uL of the final serial dilution were spotted on either YPD or the appropriate drop out plate. The plates are left to dry before incubation at the indicated temperature and for the indicated number of days of growth. Each spot dilutions have been done for a minimum of two replicates.

**Method details**

**Yeast genomic DNA isolation**

Approximately 100uL in volume of yeast were collected from a freshly streak patch and placed in a safe-lock Eppendorf tube. The cells were resuspended in 200uL of lysis buffer (10mM Tris-HCl pH 7.4, 1mM EDTA pH 8 and 3% SDS) and incubated at 65$^{o}$C for 5 minutes. Afterwards, 400uL of TE buffer was added to the samples along with 600uL of phenol-chloroform (phenol: chloroform: isoamyl alcohol 25:24:1, pH 8, Millipore Sigma). The samples were vortexed for 1

minute and centrifuged at 15,000 rpm for 5 minutes. The top aqueous layer was transferred to a new tube containing 1ml of cold 100% isopropanol to encourage the precipitation of DNA. The samples were centrifuged at 15,000 rpm for 10 minutes and the supernatant was removed. The gDNA pellet was washed once with 200uL of 70% ethanol before being resuspended in 100uL of pure water.

**RNA extraction**

To the frozen cell pellets, 500 µL of phenol: chloroform: isoamyl alcohol (25:24:1, pH 6.7, OmniPur), 400 µL of acid-washed beads and 500 µL of RNA buffer (50 mM Tris-HCl pH 7.5, 100 mM NaCl, 10mM EDTA, 2% SDS w/v ) were added and vortexed for 1 minute. The samples were incubated at 65°C for 6 minutes before being vortexed for another minute. Afterwards, the samples were spun down at 13,200 rpm for 5 minutes before 450 µL of the aqueous layer was transferred to a new Eppendorf tube containing 450 µL of fresh phenol: chloroform: isoamyl alcohol. The mixture was vortexed for an additional minute before being spun down at 15,000 rpm for 2 minutes. About 400 µL of the top aqueous layer was transferred to a new Eppendorf tube containing 1ml of 100% ethanol and 40 µL of 3M sodium acetate pH 5.2. The samples were then cooled to -80°C for 30 minutes to facilitate precipitation of the RNA. The samples are then spun down for 10 minutes at 15,000 rpm to pellet the precipitated RNA. The supernatant was then removed, and the RNA pellet washed with 200 µL of 70% ethanol. The clean RNA pellets were resuspended in 40-80 µL of nuclease-free water before being quantitated using the NanoDrop (Thermoscientific).

**Riboprobe synthesis and Oligoprobe radiolabeling for northern blot analysis**

Radiolabeled riboprobes were transcribed *in vitro* using T3 RNA polymerase (Promega) according to the manufacturer protocol. However, $\alpha$-$^{32}$P-UTP (Perkin Elmer) was used in lieu of $\alpha$-$^{32}$P-CTP. The template used in the *in vitro* transcription were synthesized through PCR using primers corresponding to the gene of interest (Table S4). After synthesis, the riboprobes are directly transferred into hybridization bottles containing the pre-hybridized membranes.

Radiolabeled oligoprobes were synthesized using a T4 polynucleotide kinase (New England Biolabs) and γ-$^{32}$P-ATP (Perkin Elmer) according to manufacturer protocol. The oligonucleotides used in this procedure can be found in the Supplemental Table S4.

**Northern Blot Analysis**

5 µg of total RNA were normalized to the same volume among all samples. The RNA aliquots were carefully combined with 4 times its volume of glyoxal buffer [60% DMSO (Sigma-Aldrich), 20% glyoxal v/v (Sigma-Aldrich), 5% glycerol, 40 µg/ml ethidium bromide, 1X BPTE pH 6.5 (10 mM PIPES (Sigma-Aldrich), 30 mM Bis-Tris (Sigma-Aldrich), 10 mM EDTA pH 8.0)] and incubated at 55$^{o}$C for 1 hour. The samples are then cooled on ice for an additional 5 minutes before being loaded onto 1.8% agarose gels made with 1X BPTE buffer. Electrophoresis was performed with 1X BPTE running buffer at 120V for 3-5 hours. After sufficient separation, the gel was washed with deionized water for 10 minutes, 75mM NaOH for 15 minutes, and in 10X SSPE buffer (100 mM sodium phosphate, 1.5 M NaCl, and 100 mM EDTA, pH 7.4) for 10 minutes. The RNA was then transferred overnight from the agarose gel to an Amersham Hybond-N$^{+}$ membrane (GE Healthcare Life Sciences) using 10X SSPE. All membranes are cross-linked with Stratalinker UV Crosslinker 2400 (Stratagene) and if necessary, stored in 2X SSPE buffer at 4°C. The membranes are pre-hybridized in Churchs buffer (1% BSA w/v, 1mM EDTA, 0.5M sodium phosphate pH 7.2, 7% SDS v/w) at 65°C for 1 hour before radiolabeled riboprobes are added directly into the buffer. The membranes are hybridized overnight before being washed twice with 2X SSPE, 0.1% SDS for 10 minutes each, and then twice with 0.1X SSPE, 0.1% SDS for 10 minutes each as well. For visualization, the washed blots are exposed to K-screens (Kodak) from several hours to up to 2 days depending on the strength of the signal. The screens are then scanned using the Bio-Rad FX Imager. Images were quantified using the Bio-Rad Quantity One Software and normalized and plotted using GraphPad.

**Western blot analysis**

Flash frozen cell pellets were lysed using a high salt lysis buffer containing 200mM Tris-HCl pH 8.0, 320mM Ammonium Sulfate, 20mM EDTA pH 8.0, 10mM EGTA pH 8.0, 5mM $MgCl_2$, 1mM DTT, 20% glycerol, 1mM PMSF and 1x protease inhibitor cocktail (Roche). Approximately 400uL of acid washed beads (Sigma) were added to the samples before being vortexed at 4°C for 3 minutes 5 times, with 1-minute breaks in between. The samples were briefly spun down and transferred to a new Eppendorf tube, leaving the glass beads behind. Cellular debris was pelleted down through centrifuging the samples at max speed for 10 minutes in a pre-chilled 4°C centrifuge. Protein concentration was quantitated using a Bradford protein assay (Bio-Rad). 5ug of protein were prepared with 1x SDS loading dye and 3.1% β-mercaptoethanol before being boiled for 5 minutes prior to loading on a 10% SDS-Page gel. After sufficient separation, the samples were transferred onto a PVDF membrane and blocked in 5% milk in PBS-T overnight at 4°C. Total and Tyr1 phosphorylated Rpb1p were detected with the RNA pol II antibody and the RNA Pol II CTD phosphor Tyr1 antibody respectively (1:5000; Active Motif). Tdh1p were detected with anti-Tdh1p antibody (Thermofisher) and Rrp6p were detected using anti-Rrp6p antibody (Wasmuth and Lima, 2017). All secondary antibodies used were obtained from LI-COR (1:10000).

**Co-immunoprecipitation**

Samples were grown and harvested as previously stated. Cell lysates were prepared as indicated above, but with the Co-IP lysis buffer (50mM Tris-HCl pH 7.4, 50mM NaCl and 1% NP-40) supplemented with protease and phosphatase inhibitors (Roche). Approximately 1.5mg of protein lysates were incubated with 25uL of magnetic anti-HA beads (Pierce) for 1 hour at 4°C. Samples were washed 6 times with lysis buffer and eluted in 40uL of 1mg/mL HA Peptide (Sigma-Aldrich). 10uL of eluate and 5ug of total lysates were loaded onto each lane of a Nu-Page gel. Rrp6p was detected with anti-Rrp6 (1:5000, (Schuch et al., 2014)) and HA tagged

proteins were detected with anti-HA (1:5000, ABM). Secondary antibodies used were obtained from LI-COR (1:10000).

**Quantification and Statistical Analysis**

**RNA-Sequencing and data analysis**

RNA-sequencing of samples was performed using biological triplicates. HISAT2 (version 2.1.0) (Kim et al., 2019) was used to align the reads to the *S. cerevisiae* reference genome (assembly 64-1-1) downloaded from Ensembl (http://ensembl.org). HTseq-count (Anders et al., 2015) (with the option -s reverse) was used with the *S. cerevisiae* genome annotation (release 97) to calculate read counts. EdgeR (version 3.26.5) (Robinson et al., 2009) was used to conduct differential gene expression analysis between the wild type and the *mpk1Δ* mutant, the wild type and *rrp6Δ* mutant, and the wild type and *mpk1Δrrp6Δ* mutants. Differentially expressed genes were selected based on the log fold change absolute value greater than 1 and the FDR q-value threshold 0.05. GO analysis was performed using GO Term Finder (version 0.86) (Boyle et al., 2004).

**KEY RESOURCES TABLE**

| REAGENT or RESOURCE | SOURCE | IDENTIFIER |
|---|---|---|
| **Antibodies** | | |
| Mouse anti-HA (clone HA.C5) | ABM | Cat #G036 |
| Rabbit anti-Rrp6 | (Wasmuth and Lima, 2017) | N/A |
| IRDye® 680RD Goat anti-Rabbit | LI-COR | Cat #926-68071 |
| IRDye® 800CW Goat anti-Mouse | LI-COR | Cat #926-32210 |
| IRDye® 680RD Goat anti-Rat | LI-COR | Cat #926-68076 |
| TDH1 Monoclonal Antibody | Thermofisher Scientific | Cat #MA5-15738 |
| RNA Pol II CTD phospho Tyr1 antibody (clone 3D12) | Active Motif | Cat #61384 |
| RNA pol II antibody (clone 4H8) | Active Motif | Cat #39497 |
| **Chemicals, Peptides, and Recombinant Proteins** | | |
| Phenol : chloroform : iso-amyl alcohol (25:24:1) | Millipore Sigma | Cat # 6810 |
| QuikChange Lightning Site-Directed Mutagenesis Kit | Agilent | Cat #210518 |
| Fast-Fusion Cloning kit | Tonkbio | Cat # TB10012A |
| Pierce™ Anti-HA Magnetic Beads | Thermofisher Scientific | Cat #88836 |
| Influenza Hemagglutinin (HA) Peptide | Sigma-Aldrich | Cat # I2149 |
| T3 RNA polymerase | Promega | Cat #P2083 |
| T4 polynucleotide kinase | New England BioLabs | Cat # M0201S |
| α-$^{32}$P-UTP | Perkin Elmer | Cat #BLU507Z001MC |
| γ-$^{32}$P-ATP | Perkin Elmer | Cat #BLU502A500UC |
| NuPAGE™ 4-12% Bis-Tris Protein Gels | Thermofisher Scientific | Cat # NP0321BOX |
| **Critical Commercial Assays** | | |
| TruSeq Stranded RNA HT Kit | Illumina | Cat#15032620 |
| **Deposited Data** | | |
| RNA-Seq of heat shocked samples | This paper | GEO: GSE140504 |
| **Experimental Models: Organisms/Strains** | | |
| ***S. cerevisiae* strains (See Table S2)** | **This paper** | **N/A** |
| **Oligonucleotides** | | |
| Plasmid construction and mutagenesis (See Table S4) | This paper | N/A |
| Probe sequence for scR1: ATCCCGGCCGCCTCCATCAC | This paper | N/A |
| Probe sequence for ITS2: AGGCCAGCAATTTCAAGTTAACTCC | This paper | N/A |
| HSP150 T3 Riboprobe (See Table S3) | This paper | N/A |
| 3xHA Tagging of Mpk1p (See Table S3) | This paper | N/A |
| **Recombinant DNA** | | |
| Plasmids transformed in *S. cerevisiae* (See Table S3) | This paper | N/A |
| **Software and Algorithms** | | |
| HISAT2 | (Kim et al., 2019) | RRID:SCR_015530 |
| HTseq-count | (Anders et al., 2015) | RRID:SCR_011867 |
| edgeR | (Robinson et al., 2009) | RRID:SCR_012802 |
| GO Term Finder | (Boyle et al., 2004) | RRID:SCR_008870 |

**Supplemental Figure Legends**

**Figure S1. Disabling cytoplasmic RNA processing and degradation factors does not cause lethality in the *mpk1Δ* mutant. Related to Figure 1.**

Indicated strains were serially diluted and spotted onto YPD plates and incubated at 30°C or 37°C for the number of days indicated.

**Figure S2. Western blot analysis of Rrp6p and Mpk1p and rRNA processing in Rrp6p mutants. Related to Figure 2**. (A) Western blot analysis of Rrp6p levels in various exosome mutants grown at steady state 37°C. (B-D) Western blot analysis depicting similar protein levels of Rrp6p mutants and Mpk1p mutants before and after heat shock. An HA-tag was used to detect Mpk1p, while Rrp6p was detected using anti-Rrp6p antibodies (gift of C.Lima). (E-F) Northern blot analysis showing rRNA processing defects in the Rrp6p-D238N and Rrp6p-TAP strains. The 27S and 7S rRNAs intermediates were detected using an oligoprobe targeting the ITS2 region. scR1 was used as a loading control.

**Figure S3. Genetic interactions between Rrp6p and components of the CWI pathway. Related to Figure 3.**

(A-C) Serial dilution assay of the indicated strains grown on YPD or SD-URA plates. The plates were incubated at 30°C or 37°C and for the number of days indicated.

**Figure S4. Rrp6p does not interact stably with Mpk1p or alter Tyr1 phosphorylation of the RNAPII CTD. Related to Figures 4 and 5.**

(A) Co-IP detecting no stable interaction between Mpk1-HA and Rrp6p. (B) Immunoblot indicating no changes in the Tyr1 phosphorylation of the CTD of Rpb1p in the indicated strains.

# Figure 1 - Wang et al.

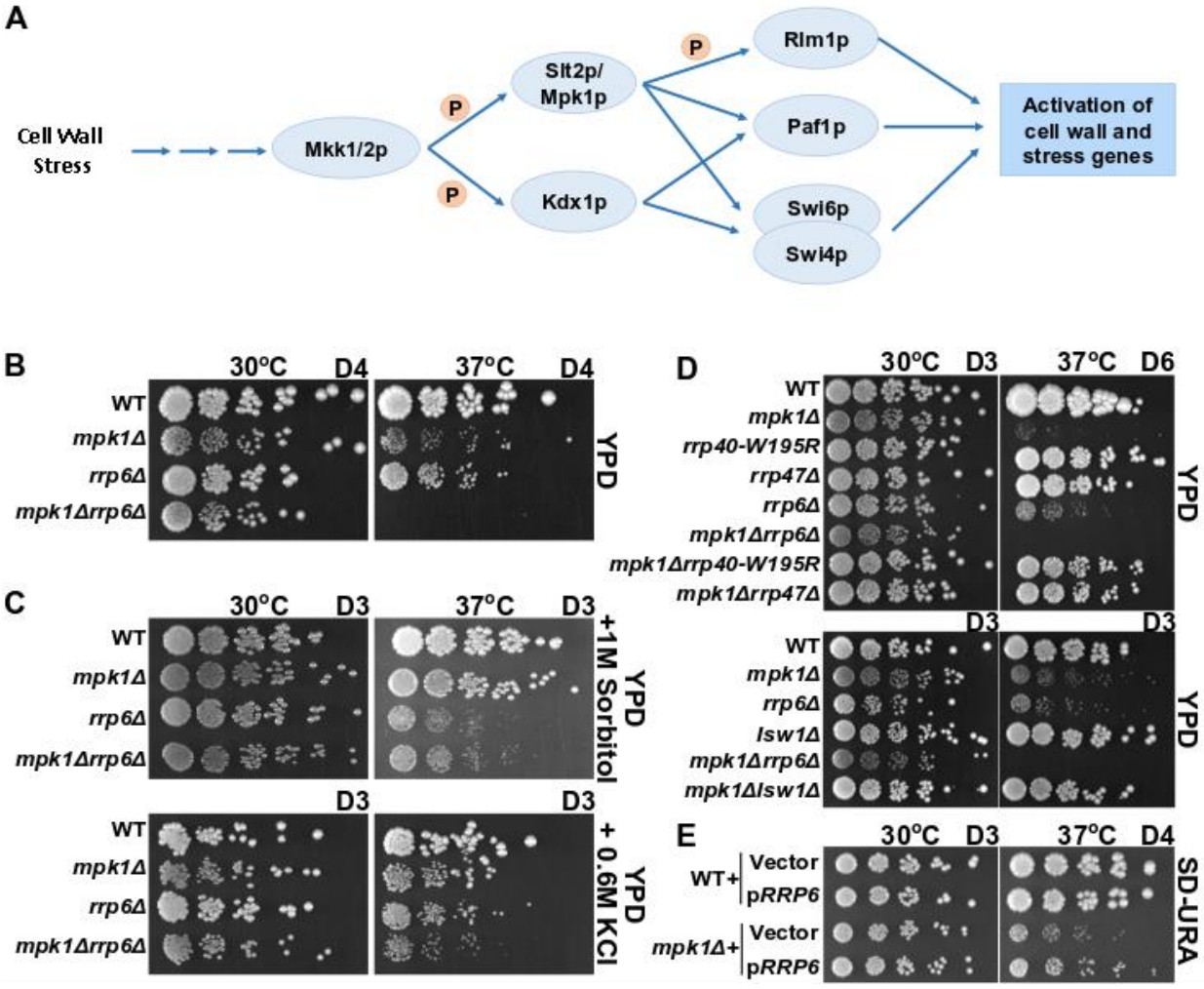

# Figure 2 - Wang et al.

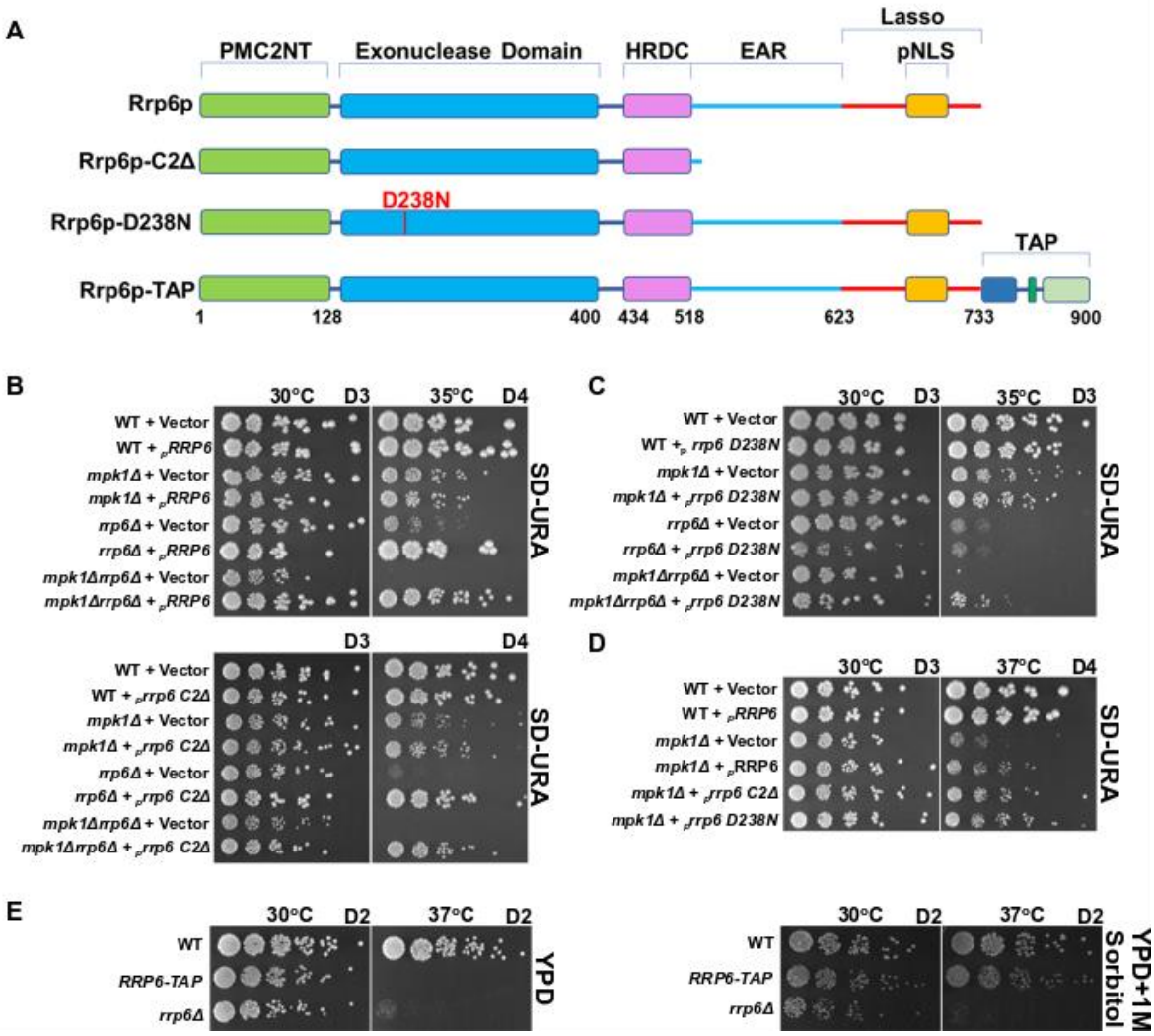

**Figure 3 - Wang et al.**

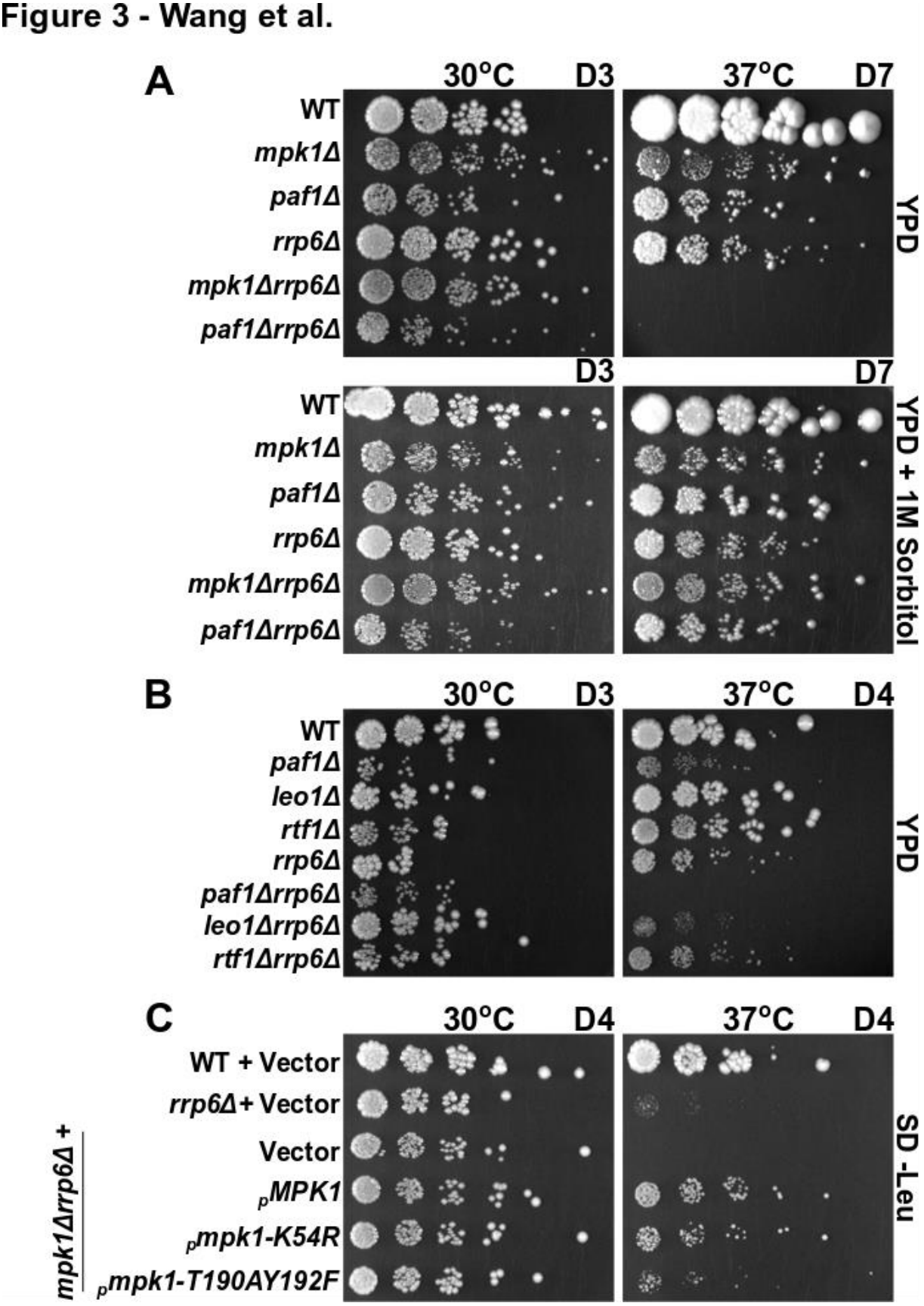

# Figure 4 - Wang et al.

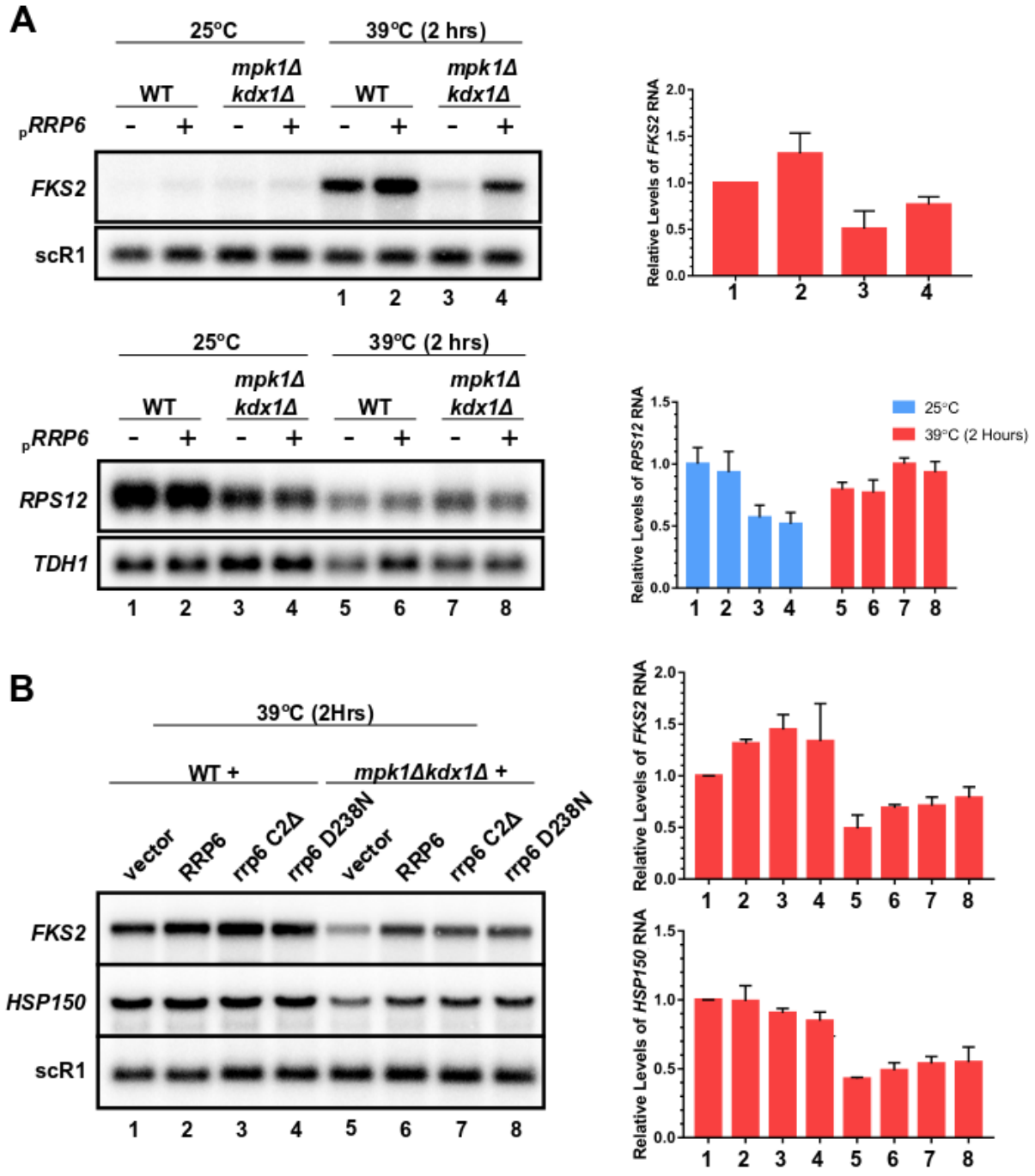

**Figure 5 - Wang et al.**

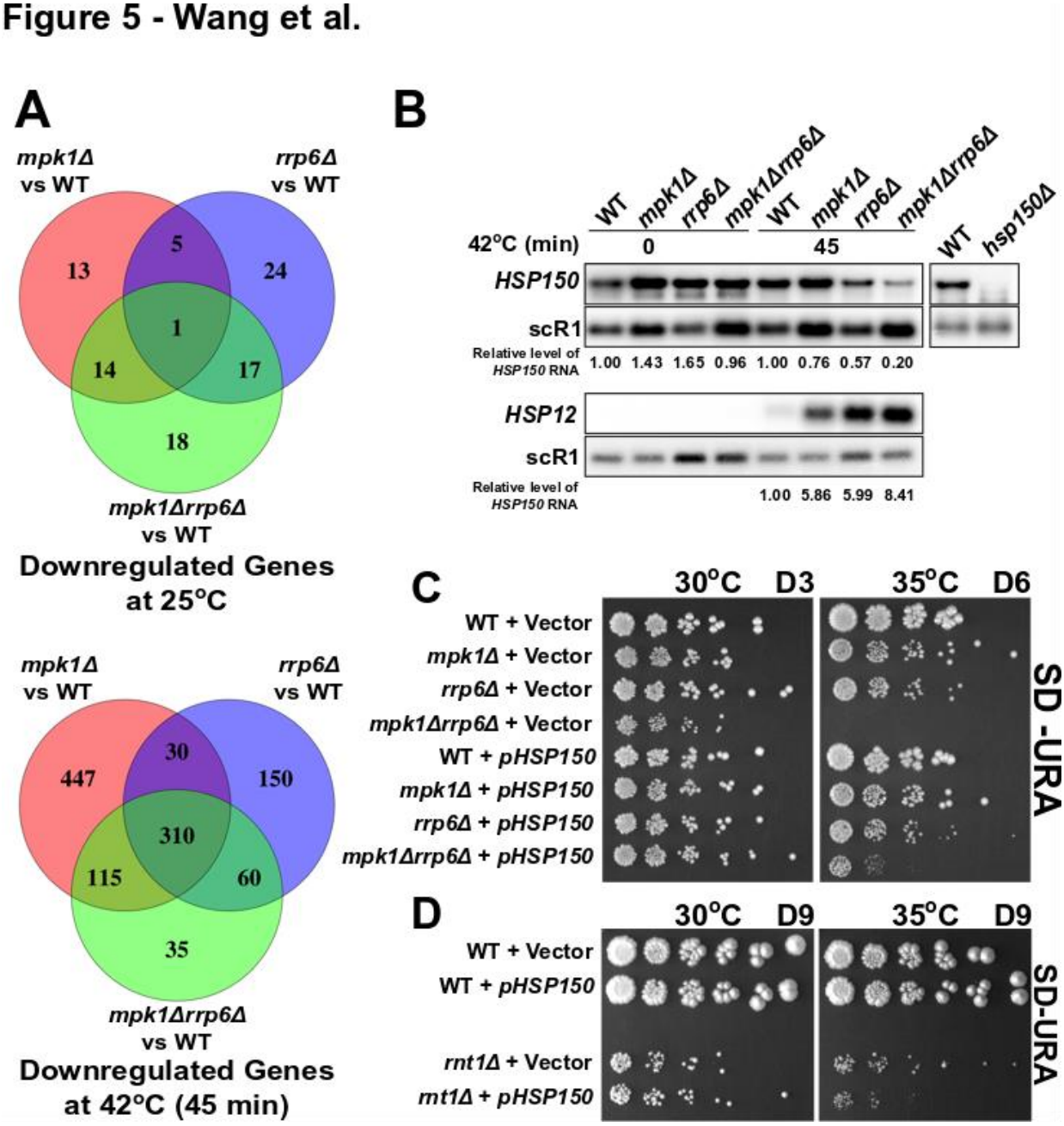

**Figure S1 - Wang et al.**

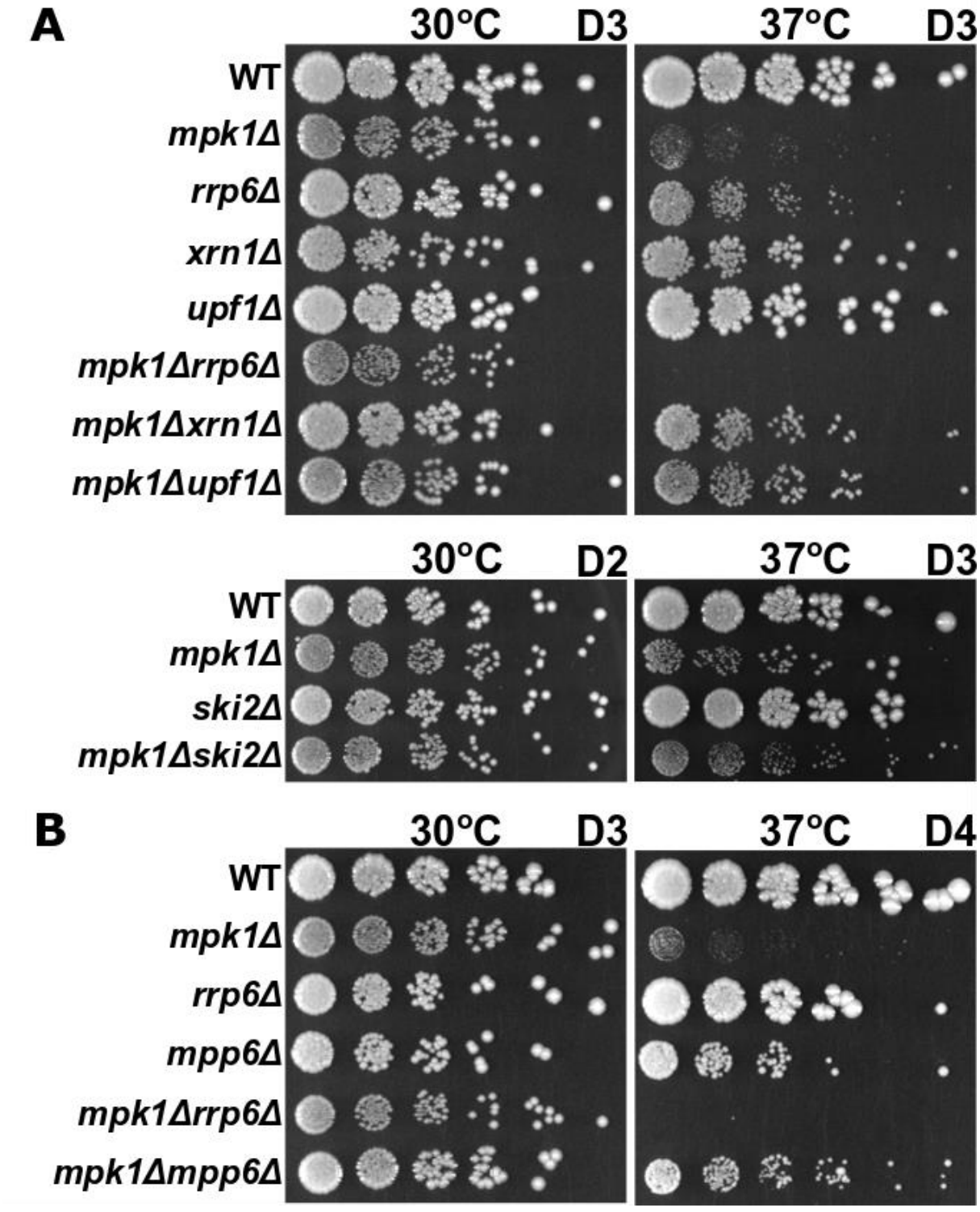

# Figure S2 - Wang et al.

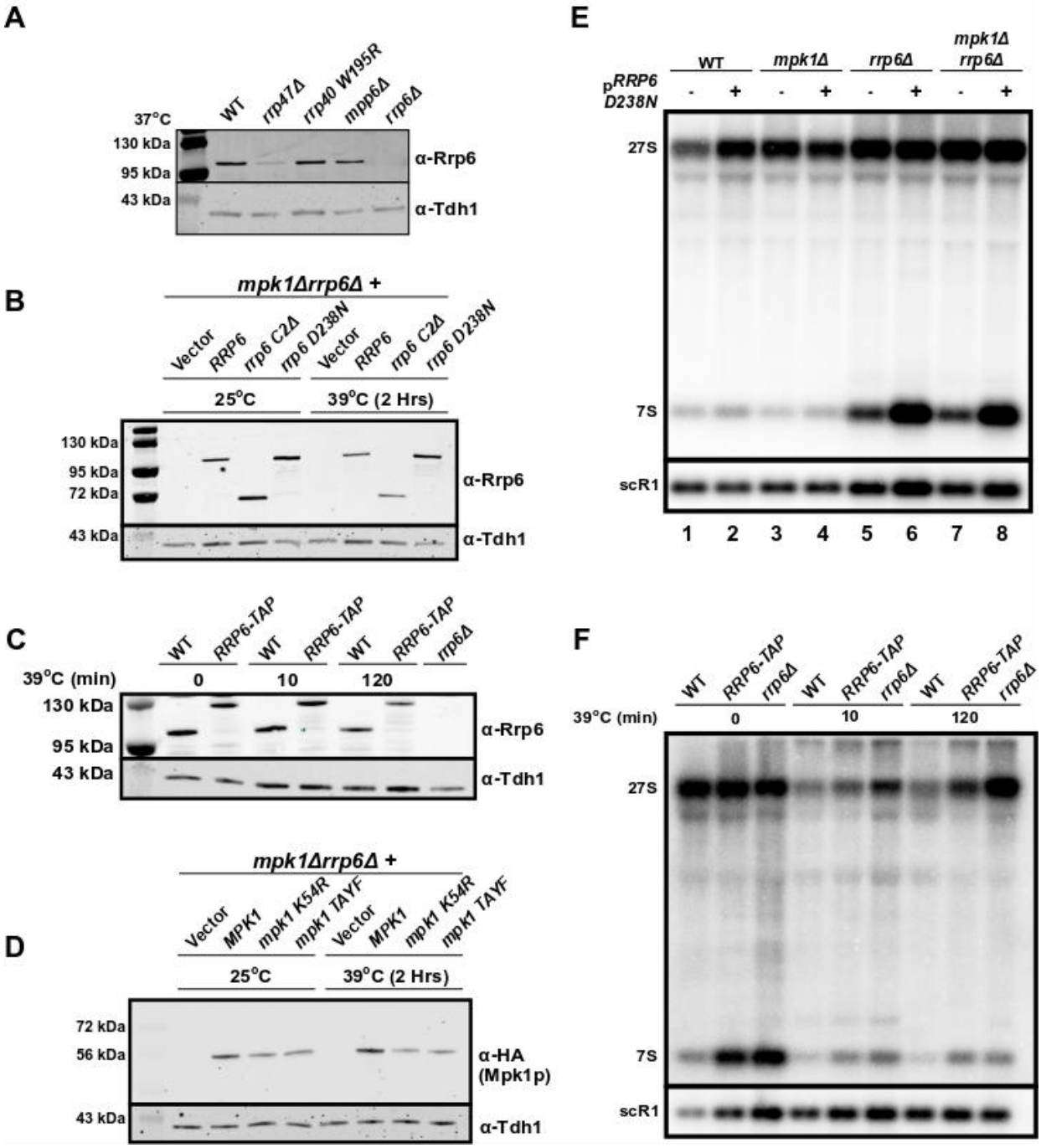

**Figure S3 - Wang et al.**

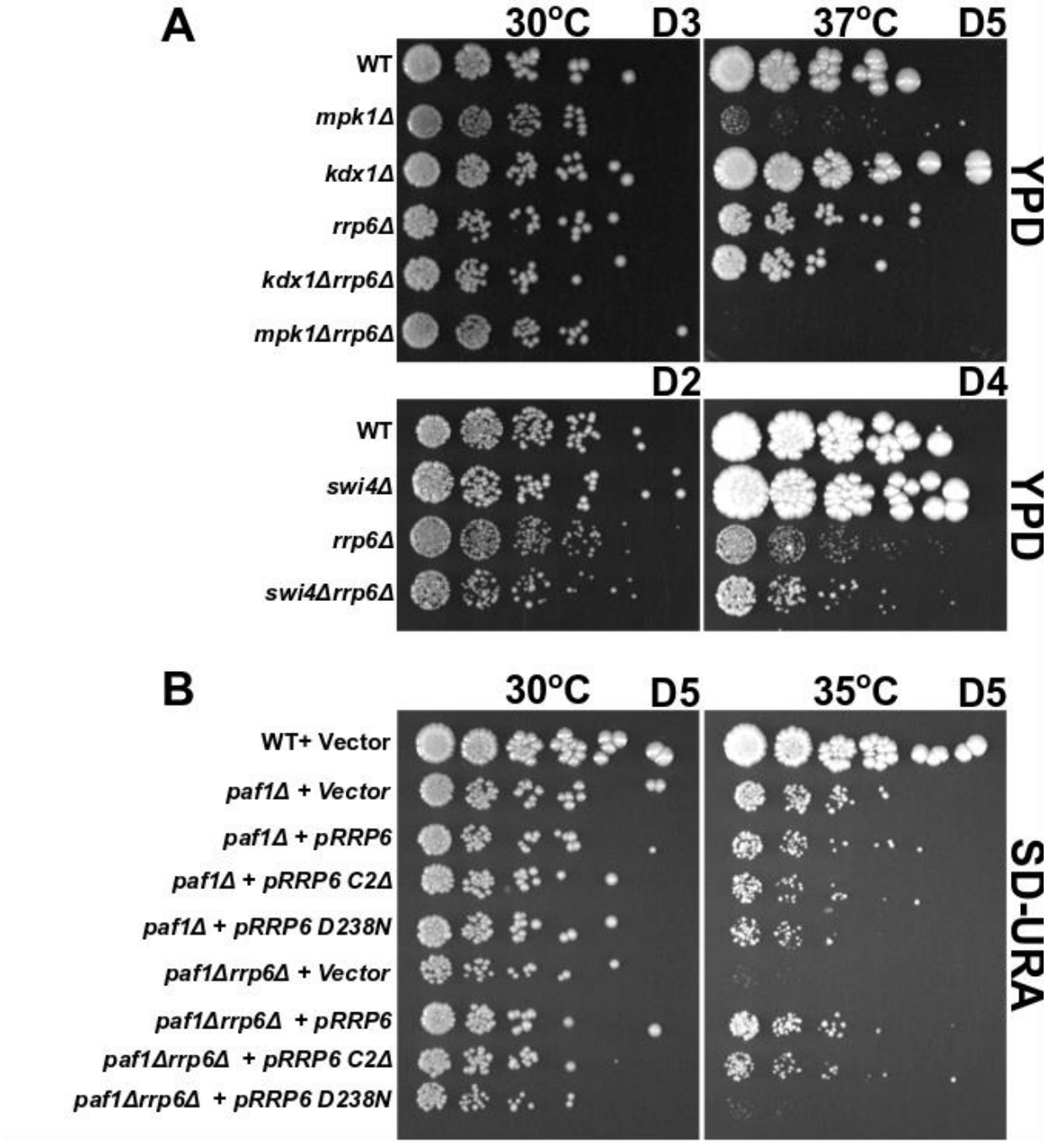

# Figure S4 - Wang et al.

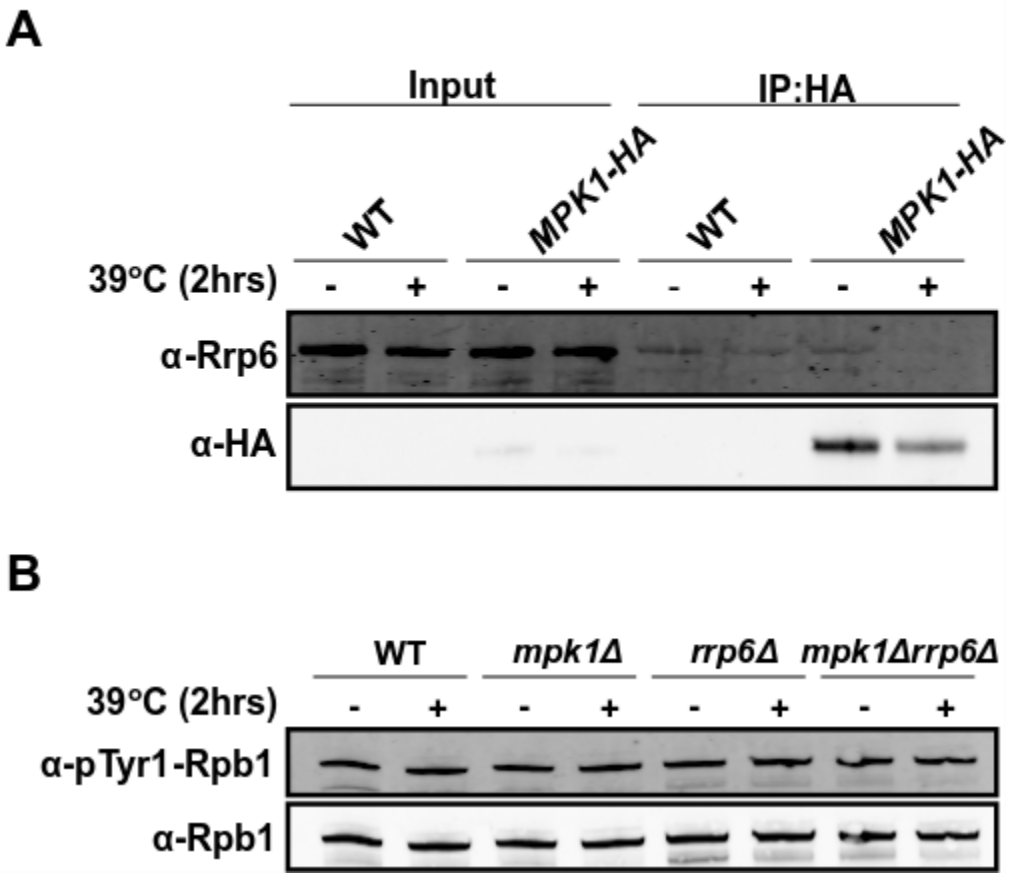

**References**

Allmang, C., Kufel, J., Chanfreau, G., Mitchell, P., Petfalski, E., and Tollervey, D. (1999). Functions of the exosome in rRNA, snoRNA and snRNA synthesis. EMBO J. *18*, 5399–5410.

Anders, S., Pyl, P.T., and Huber, W. (2015). HTSeq-A Python framework to work with high-throughput sequencing data. Bioinformatics *31*, 166–169.

Andrulis, E.D., Werner, J., Nazarian, A., Erdjument-Bromage, H., Tempst, P., and Lis, J.T. (2002). The RNA processing exosome is linked to elongating RNA polymerase II in Drosophila. Nature *420*, 837–841.

Babour, A., Shen, Q., Dos-Santos, J., Murray, S., Gay, A., Challal, D., Fasken, M., Palancade, B., Corbett, A., Libri, D., et al. (2016). The Chromatin Remodeler ISW1 Is a Quality Control Factor that Surveys Nuclear mRNP Biogenesis. Cell *167*, 1201-1214.e15.

Bernstein, J., and Toth, E.A. (2012). Yeast nuclear RNA processing. World J. Biol. Chem. *3*, 7–26.

Boyle, E.I., Weng, S., Gollub, J., Jin, H., Botstein, D., Cherry, J.M., and Sherlock, G. (2004). GO::TermFinder - Open source software for accessing Gene Ontology information and finding significantly enriched Gene Ontology terms associated with a list of genes. Bioinformatics *20*, 3710–3715.

Bresson, S., Tuck, A., Staneva, D., and Tollervey, D. (2017). Nuclear RNA Decay Pathways Aid Rapid Remodeling of Gene Expression in Yeast. Mol. Cell *65*, 787-800.e5.

Brul, S., Ruiz, C., Morris, W., Klis, F.M., Molina, M., de Nobel, H., and Martin, H. (2000). Cell wall perturbation in yeast results in dual phosphorylation of the Slt2/Mpk1 MAP kinase and in an Slt2-mediated increase in FKS2–lacZ expression, glucanase resistance and thermotolerance. Microbiology *146*, 2121–2132.

Burkard, K.T., and Butler, J.S. (2000). A nuclear 3’-5’ exonuclease involved in mRNA degradation interacts with Poly(A) polymerase and the hnRNA protein Npl3p. Mol. Cell. Biol. *20*, 604–616.

Butler, J.S., and Mitchell, P. (2010). Rrp6, Rrp47 and cofactors of the nuclear exosome. Adv. Exp. Med. Biol. *702*, 91–104.

Callahan, K.P., and Butler, J.S. (2008). Evidence for core exosome independent function of the nuclear exoribonuclease Rrp6p. Nucleic Acids Res. *36*, 6645–6655.

Carmody, S.R., Tran, E.J., Apponi, L.H., Corbett, A.H., and Wente, S.R. (2010). The Mitogen-Activated Protein Kinase Slt2 Regulates Nuclear Retention of Non-Heat Shock mRNAs during Heat Shock-Induced Stress. Mol. Cell. Biol. *30*, 5168–5179.

Fasken, M.B., Losh, J.S., Leung, S.W., Brutus, S., Avin, B., Vaught, J.C., Potter-Birriel, J., Craig, T., Conn, G.L., Mills-Lujan, K., et al. (2017). Insight into the RNA Exosome Complex Through Modeling Pontocerebellar Hypoplasia Type 1b Disease Mutations in Yeast. Genetics *205*, 221–237.

Feigenbutz, M., Jones, R., Besong, T.M.D., Harding, S.E., and Mitchell, P. (2013a). Assembly of the yeast exoribonuclease Rrp6 with its associated cofactor Rrp47 occurs in the nucleus and is critical for the controlled expression of Rrp47. J. Biol. Chem. *288*, 15959–15970.

Feigenbutz, M., Garland, W., Turner, M., and Mitchell, P. (2013b). The exosome cofactor Rrp47 is critical for the stability and normal expression of its associated exoribonuclease Rrp6 in Saccharomyces cerevisiae. PLoS One *8*, e80752.

Fox, M.J., and Mosley, A.L. (2016). Rrp6: Integrated roles in nuclear RNA metabolism and transcription termination. Wiley Interdiscip. Rev. RNA *7*, 91–104.

Fox, M.J., Gao, H., Smith-Kinnaman, W.R., Liu, Y., and Mosley, A.L. (2015). The Exosome Component Rrp6 Is Required for RNA Polymerase II Termination at Specific Targets of the Nrd1-Nab3 Pathway. PLoS Genet. *11*, 1–26.

Gietz, R.D., and Schiestl, R.H. (2007). High-efficiency yeast transformation using the LiAc/SS carrier DNA/PEG method. Nat. Protoc. *2*, 31–34.

Gillespie, A., Gabunilas, J., Jen, J.C., and Chanfreau, G.F. (2017). Mutations of EXOSC3/Rrp40p associated with neurological diseases impact ribosomal RNA processing

functions of the exosome in S. cerevisiae. RNA *23*, 466–472.

Graham, A.C., Kiss, D.L., and Andrulis, E.D. (2009). Core Exosome-independent Roles for Rrp6 in Cell Cycle Progression. Mol. Biol. Cell *20*, 2242–2253.

Gustin, M.C., Albertyn, J., Alexander, M., and Davenport, K. (1998). MAP kinase pathways in the yeast Saccharomyces cerevisiae. Microbiol. Mol. Biol. Rev. *62*, 1264–1300.

Hahn, J.-S., and Thiele, D.J. (2002). Regulation of the Saccharomyces cerevisiae Slt2 kinase pathway by the stress-inducible Sdp1 dual specificity phosphatase. J. Biol. Chem. *277*, 21278–21284.

Jin, C., Strich, R., and Cooper, K.F. (2014). Slt2p phosphorylation induces cyclin C nuclear-to-cytoplasmic translocation in response to oxidative stress. Mol. Biol. Cell *25*, 1396–1407.

Kanehisa, M., and Goto, S. (2000). KEGG: kyoto encyclopedia of genes and genomes - Release 72.1, December 1, 2014 . Nucleic Acids Res *28*, 27–30.

Kim, K.-Y., and Levin, D.E. (2011). Mpk1 MAPK association with the Paf1 complex blocks Sen1-mediated premature transcription termination. Cell *144*, 745–756.

Kim, D., Paggi, J.M., Park, C., Bennett, C., and Salzberg, S.L. (2019). Graph-based genome alignment and genotyping with HISAT2 and HISAT-genotype. Nat. Biotechnol. *37*, 907–915.

Kim, K.-Y., Truman, A.W., Caesar, S., Schlenstedt, G., and Levin, D.E. (2010). Yeast Mpk1 cell wall integrity mitogen-activated protein kinase regulates nucleocytoplasmic shuttling of the Swi6 transcriptional regulator. Mol. Biol. Cell *21*, 1609–1619.

Levin, D.E. (2005). Cell wall integrity signaling in Saccharomyces cerevisiae. Microbiol. Mol. Biol. Rev. *69*, 262–291.

Longtine, M.S., Mckenzie III, A., Demarini, D.J., Shah, N.G., Wach, A., Brachat, A., Philippsen, P., and Pringle, J.R. (1998). Additional modules for versatile and economical PCR-based gene deletion and modification in Saccharomyces cerevisiae. Yeast *14*, 953–961.

Moraes, K.C.M. (2010). RNA surveillance: molecular approaches in transcript quality control and their implications in clinical diseases. Mol. Med. *16*, 53–68.

Morton, D.J., Kuiper, E.G., Jones, S.K., Leung, S.W., Corbett, A.H., and Fasken, M.B. (2018). The RNA exosome and RNA exosome-linked disease. RNA *24*, 127–142.

Van Oss, S.B., Cucinotta, C.E., Arndt, K.M., Branden, S., Oss, V., Cucinotta, C.E., and Arndt, K.M. (2017). Emerging Insights into the Roles of the Paf1 Complex in Gene Regulation. Trends Biochem. Sci. *42*, 788–798.

Parker, R. (2012). RNA degradation in Saccharomyces cerevisae. Genetics *191*, 671–702.

Robinson, M.D., McCarthy, D.J., and Smyth, G.K. (2009). edgeR: A Bioconductor package for differential expression analysis of digital gene expression data. Bioinformatics *26*, 139–140.

Russo, P., Kalkkinen, N., Sareneva, H., Paakkola, J., and Makarow, M. (1992). A heat shock gene from Saccharomyces cerevisiae encoding a secretory glycoprotein. Proc. Natl. Acad. Sci. U. S. A. *89*, 3671–3675.

Schuch, B., Feigenbutz, M., Makino, D.L., Falk, S., Basquin, C., Mitchell, P., and Conti, E. (2014). The exosome-binding factors Rrp6 and Rrp47 form a composite surface for recruiting the Mtr4 helicase. EMBO J. *33*, 2829–2846.

Sloan, K.E., Schneider, C., and Watkins, N.J. (2012). Comparison of the yeast and human nuclear exosome complexes. Biochem. Soc. Trans. *40*, 850–855.

Volanakis, A., Passoni, M., Hector, R.D., Shah, S., Kilchert, C., Granneman, S., and Vasiljeva, L. (2013). Spliceosome-mediated decay (SMD) regulates expression of nonintronic genes in budding yeast. Genes Dev. *27*, 2025–2038.

Wan, J., Yourshaw, M., Mamsa, H., Rudnik-Schöneborn, S., Menezes, M.P., Hong, J.E., Leong, D.W., Senderek, J., Salman, M.S., Chitayat, D., et al. (2012). Mutations in the RNA exosome component gene EXOSC3 cause pontocerebellar hypoplasia and spinal motor neuron degeneration. Nat. Genet. *44*, 704–708.

Wasmuth, E. V, and Lima, C.D. (2017). The Rrp6 C-terminal domain binds RNA and activates the nuclear RNA exosome. Nucleic Acids Res. *45*, 846–860.

Yurko, N., Liu, X., Yamazaki, T., Hoque, M., Tian, B., and Manley, J.L. (2017). MPK1/SLT2

Links Multiple Stress Responses with Gene Expression in Budding Yeast by Phosphorylating Tyr1 of the RNAP II CTD. Mol. Cell *68*, 913–925.

Zinder, J.C., and Lima, C.D. (2017). Targeting RNA for processing or destruction by the eukaryotic RNA exosome and its cofactors. Genes Dev. *31*, 88–100.

# Chapter 3

## Inhibition of mRNA export triggers Rnt1 mediated decay of the *BDF2* mRNA

## Abstract

Bromodomain factors have emerged as key transcriptional regulators due to their roles in controlling chromatin remodeling and transcription. Because of their impact on eukaryotic transcriptomes, their expression is tightly controlled to ensure the appropriate modulation of gene expression. In the yeast *S. cerevisiae*, Bromodomain Factor 2 (*BDF2)* expression is extensively regulated post-transcriptionally by both RNase III-mediated decay (RMD) and spliceosome-mediated decay (SMD). Previous studies have shown that RMD-mediated down-regulation of *BDF2* is hyper-activated in osmotic stress conditions, yet the mechanisms driving the enhanced cleavage of *BDF2* RNA under these conditions remain unknown. In this study we show that RMD-mediated down-regulation of *BDF2* transcripts can be detected in a variety of stress conditions, and that RNase III cellular localization remains unchanged during stress. We further show that inhibiting the nuclear export of *BDF2* transcripts by anchoring away mRNA export or cleavage and polyadenylation factors can recapitulate the stress-induced RMD hyper-activation. Consistent with the nuclear retention of *BDF2* transcripts during stress, driving RNase III out of the nucleus is sufficient to abrogate *BDF2* RMD activity. Because several stress conditions are known to mediate global inhibition of mRNA export, these results suggest that the hyperactivation of *BDF2* RMD during stress is primarily due to the increased nuclear retention of *BDF2* mRNA. This leads to an increased exposure of *BDF2* transcripts to RNase III cleavage. The efficiency of cleavage may further contribute to the sensitivity of these transcripts to degradation. Taken together, we provide evidence of Rnt1p regulating transcript abundance based on the transcript's localization and stem loop sequence.

## Introduction

Epigenetics is a tool commonly utilized by the cells to integrate environmental stress signals with gene expression. This process ultimately enhances or restrains expressions of specific genes. One common epigenetic mechanism, the covalent modification of histones,

affects the accessibility of DNA for damage repair, transcriptional activation or repression and heterochromatin formation (Lawrence et al., 2016). The acetylation of histones is a well-studied covalent modification that is generally associated with transcriptional activation (Kurdistani & Grunstein, 2003). Bromodomain-containing proteins bind to acetylated histones and recruits various proteins to alter gene expression (Josling et al., 2012). As so, they are key players in transcription regulation.

Bromodomain factor 2 (Bdf2p) is one of the two bromodomain-containing proteins that recognizes acetylated lysines on histones. Bdf2p has been found to establish heterochromatin boundaries and regulate the yeast salt stress response, although the specific mechanisms that govern these processes remain elusive (Fu et al., 2013). Bdf2p is not essential for growth. However, its absence along with its homolog Bdf1p is shown to be inviable in yeast (Matangkasombut et al., 2000). This suggests that there is partial redundancy between the functions of the two proteins. Indeed, the overexpression of *BDF2* rescues the salt sensitivity and mitochondrial dysfunction of *bdf1Δ* mutants (Fu et al., 2013). This functional redundancy is further confirmed by the observation that Bdf2p will occupy empty Bdf1p binding sites in mutants lacking Bdf1p (Durant & Pugh, 2007). The absence of Bdf1p also increases the basal expression of *BDF2* by three fold (Fu et al., 2013; Volanakis et al., 2013). Interesting, Bdf2p has been found to interact with the transcription factor II D (TFIID) complex, implicating a possible wider role in regulating transcription (Fu et al., 2013; Matangkasombut et al., 2000). These observations show that the regulation of *BDF2* expression is necessary to balance its expression relative to that of *BDF1*, and to control its expression during stress.

Post-transcriptional regulation of *BDF2* expression is achieved through two distinct pathways; spliceosome-mediated decay (SMD) (Volanakis et al., 2013) and RNase III-mediated decay (RMD) (Roy & Chanfreau, 2014). Interestingly, these two distinct degradation pathways

are activated by different environmental stresses for *BDF2* transcripts. During osmotic stress, RMD predominates over SMD while the opposite is true during DNA damage stress conditions (Roy & Chanfreau, 2014). The increase in the activity, or hyper-activation, of RMD during salt stress results in a drastic decrease of the available pool of *BDF2* transcripts. However, the mechanism by which RMD is hyperactivated during stress remains unknown. In this study, we provide evidence that the increased cleavage of the *BDF2* transcripts during specific stress conditions is due to increased *BDF2* transcripts retention within the nucleus. These results show that RMD can act as an additional layer in regulating gene expression, where undesirable transcripts are retained within the nucleus and subsequently degraded by RMD.

## Results

### Rnt1p protein levels remain stable in salt stress

Previous studies have shown that the *BDF2* mRNA can be regulated by both spliceosome mediated decay (SMD) (Volanakis et al., 2013) as well as RNase III-mediated decay (RMD) pathways (Roy & Chanfreau, 2014). In the presence of high concentrations of NaCl, RMD dominates over SMD and causes significant degradation of the *BDF2* transcript (Roy & Chanfreau, 2014). This results in a decrease of the full length *BDF2* transcript and a simultaneous increase of the 5' *BDF2* cleavage fragment (Figure 2C). The resulting 5' cleavage fragment is readily detectable by northern blot analysis despite its active removal by the nuclear exosome. To further investigate the mechanism responsible for RMD hyper-activation on the *BDF2* transcript in NaCl stress, we first analyzed the Rnt1p protein levels through western blot analysis, as increased Rnt1p expression or modulation of its activity by post-translational modifications might result in increased RNase III cellular activity. The resolving gel was supplemented with Phos-tag to enhance the separation of non-phosphorylated Rnt1p from its phosphorylated form (Nagy et al., 2018). Western blot analysis showed no clear difference of the Rnt1p protein levels between samples grown in normal medium versus those treated with

high salt (Figure 1A). This suggests that the RMD hyper-activation seen on the *BDF2* transcript is not a consequence of an overall increase of Rnt1p protein in salt stress. In addition, a lack of difference in the migration rates between the samples further suggests that the phosphorylation state of Rnt1p remains identical during salt stress.

**Rnt1p remains localized in the nucleus during salt stress and its nuclear localization is necessary for *BDF2* RMD.**

Rnt1p is exclusively localized in the nucleoplasm and nucleolus (Catala et al., 2004; Henras et al., 2004). However, it is unknown if the subcellular localization of Rnt1p changes during stress or under different environmental conditions. We hypothesized that if the bulk of the *BDF2* mRNA is cytoplasmic, an increase of Rnt1p localization in the cytoplasm during osmotic stress may result in an increase in the *BDF2* mRNA RMD. In order to visualize the localization of Rnt1p within the cell, we utilized fluorescence microscopy of a GFP-tagged Rnt1p, which was shown in previous studies to be functional (Henras et al., 2004). We did not observe a difference in the subcellular localization of Rnt1p in strains treated with or without high salt (Figure 1B). This observation suggests that the Rnt1p mediated cleavage of *BDF2* transcripts must occur within the nucleus. To further show that the nuclear localization of Rnt1p is necessary for *BDF2* mRNA RMD, we nuclear depleted Rnt1p through the anchor away technique (Haruki et al., 2008). The absence of Rnt1p from the nucleus is sufficient in preventing *BDF2* transcript cleavage, supporting our data that RMD predominantly occurs within the nucleus (Figure 1C). Interestingly, this experiment also showed that some of the *BDF2* transcripts undergo RMD during standard growth, as shown by an increase in the *BDF2* transcript abundance after the nuclear depletion of Rnt1p. Altogether, our data shows that RMD is dependent on the nuclear localization of Rnt1p and that this localization remains unaltered in salt stress.

Previous studies have shown that environmental stresses may causes global poly(A)$^+$ mRNA retention within the nucleus (Izawa et al., 2008; Peter W. Piper, 1995; C. Saavedra et al., 1996). As so, it is conceivable that salt stress may cause a similar global poly(A)$^+$ mRNA retention behavior as a mechanism to overcome the stress. In this scenario, nuclear retained transcripts would be more likely to undergo RMD. Using Cy3-labeled oligo d(T)$_{50}$ to visualize all polyadenylated mRNA through fluorescence *in situ* hybridization (FISH), a distinct pattern of nuclear poly(A)$^+$ mRNA aggregation can be seen after salt stress (Figure 1B). We tried to specifically detect BDF2 localization by FISH in these conditions, but we were not able to obtain consistent data using oligonucleotide probes complementary to the BDF2 sequence (not shown). Taken together, our data show that high salt stress does not induce an overall change in the nuclear localization of Rnt1p. However, salt stress does result in an overall change in the localization behavior of poly(A)$^+$ mRNAs that may contribute towards different RMD activity.

**_BDF2_ RMD hyperactivation can be detected in a variety of stress conditions that are known to result in mRNA nuclear retention.**

The previous data showed that nuclear localization of Rnt1p is necessary for the cleavage of *BDF2* transcripts, suggesting that an increase of *BDF2* mRNA nuclear retention during salt stress may be the primary mechanism for RMD hyperactivation. To further test this hypothesis, we subjected *S. cerevisiae* to various stresses and analyzed the *BDF2* transcript through northern blotting. Ethanol or heat shock stress, are known to cause selective retention of bulk mRNAs within the nucleus and the rapid export of stress responsive transcripts (Figure 2A) (Izawa et al., 2008; P. W. Piper et al., 1994; C. A. Saavedra et al., 1997). Strikingly, we detected RMD hyperactivation on *BDF2* in cells treated with ethanol or heat shock. Ethanol treatment results in a progressive increase of RMD activity on *BDF2* mRNA overtime, as shown through a decrease of the full-length transcript. However, the opposite is true for heat shocked samples, where the cleavage fragment was detected at its peak within the first 10 minutes of

treatment. No cleavage fragment was detected after an hour of heat shock, as the cells may have recovered from the stress. Interestingly, a complete loss of the full length *BDF2* transcript was not seen during salt treatment at 23˚C, as compared to salt treatment as 30˚C. This suggests that the steady state growth temperature may influence the cleavage activity of Rnt1p as well. Nonetheless, these data using heat shock and ethanol stress treatments support the notion that the RMD hyperactivation seen on *BDF2* mRNAs may be due to the retention of these transcripts being subjected to additional cleavage by Rnt1p. In addition, we detected a progressive increase of *BDF2* mRNA RMD with increasing concentration of either lithium chloride or sodium chloride (Figure 2B). No full length *BDF2* can be observed after an hour of 0.6M lithium chloride or sodium chloride treatment. Furthermore, the absence of cleavage in the 1 M or 2M Sorbitol treatment suggests that the RMD hyper-activation on *BDF2* in salt stress is primarily due to ionic stress and not osmotic stress. We further explored the type of ionic stress that can mediate RMD of *BDF2*. We found that the addition of high KCl concentrations did not activate RMD, indicating that RMD hyper-activation is specific to the type of ionic stress (Figure 2C). A similar result was obtained when nuclear exosome activity was impaired by the deletion of Rrp6p to ensure that any cleavage activity is not masked by the degradation of the cleavage product (Figure 2C). Altogether, these results demonstrate that *BDF2* RMD can be hyper-activated in various stress conditions but that the RMD activation is specific to particular stress conditions known to induce mRNA nuclear retention.

**BDF2 RMD hyperactivation can be recapitulated by anchoring away cleavage and polyadenylation or mRNA export factors.**

To confirm the possibility that the RMD hyperactivation on *BDF2* is due to the transcript's nuclear retention, we tested the effect of inhibiting mRNA export to the cytoplasm. The anchor-away technique (Haruki et al., 2008) was used to rapidly deplete several proteins from the nucleus that are involved directly or indirectly in the export of mRNAs to the cytoplasm. We first

focused on the Nab2p, Nab4p (Hrp1p), Yth1p, and Ysh1p cleavage and polyadenylation (CPA) factors, as 3'-end processing of mRNAs is necessary for efficient mRNA export (Guisbert et al., n.d.; Hammell et al., 2002). For all these proteins, a robust cleavage of *BDF2* transcripts was detected in the absence of any stress conditions shortly after anchoring away these CPA factors (Figure 3A and B). This suggests that the inhibition of mRNA export by CPA inhibition is sufficient to recapitulate the salt stress induced RMD hyper-activation on *BDF2* mRNA. However, the degree of cleavage activity upon anchoring away CPA factors did not reach the same extent to that of salt stress. Although a decrease of the full length *BDF2* transcript can be seen after anchoring away Nab2p, Ysh1p and Yth1, a complete loss of the full-length transcript was observed after salt treatment (Figure 3A and B). Moreover, a further decrease of the *BDF2* full-length transcript, and a corresponding increase of its cleavage fragment, was detected after the addition of salt stress to the nuclear depleted CPA strains. This additive effect may either indicate a synergy between the retention of unprocessed RNAs and the retention of mRNAs during stress for RMD activation, or that the anchoring away of a single CPA factor may not completely abolish mRNA export. Interestingly, the anchoring away Nab4p, Ysh1p and Yth1p resulted in the appearance of several transcripts larger than the full length *BDF2* mRNA (Figure 3A and B). These extended species may be attributed to transcription termination defects arising from a defective CPA machinery (Minvielle-Sebastia et al., 1998)

To further assess the link between RMD hyper-activation and nuclear export, we performed nuclear depletion of the principal mRNA export factor, Mex67p. Mex67p is a core member of the mRNA export complex and its nuclear depletion through the anchor-away technique completely abolishes poly(A)$^+$ mRNA export (Haruki et al., 2008). Strikingly, the nuclear depletion of Mex67p is sufficient to fully induce RMD hyper-activation on *BDF2* (Figure 3C). In fact, the nuclear depletion of Mex67p results in a complete loss of the full length *BDF2* transcripts, a phenotype stronger than the nuclear depletion of 3'-end processing factors. The

complete cleavage of the *BDF2* transcripts is further confirmed as no additional cleavage product accumulates when the nuclear depleted samples were treated with salt stress. Thus, these results indicate that the subcellular localization of *BDF2* mRNAs play a pivotal role in determining their degradation fate through RMD, and that inhibition of mRNA nuclear export can fully recapitulate RMD hyperactivation of *BDF2* transcripts.

**Identity of promoter does not influence *BDF2* RMD hyper-activation**

Elements within the promoter of transcripts may affect their overall mRNA stability (Catala & Abou Elela, 2019; Trcek et al., 2011). This promoter-dependent regulation of mRNA stability was shown to be controlled through the recruitment of several proteins that initiate mRNA decay. Rnt1p itself can be recruited to the promoter before being translocated to its recognition stem loop within the ORF for cleavage (Catala & Abou Elela, 2019). To determine if the RMD hyper-activation of the *BDF2* mRNA relies on the recruitment of Rnt1p to its promoter, we swapped its promoter with that of *HSP12.* The *HSP12* mRNA does not undergo RMD and as so, we expect that its promoter will be unable to recruit Rnt1p despite containing many stress response elements (STRE) (Varela et al., 1995). Furthermore, the *HSP12* promoter is highly active under salt stress, allowing us to visualize whether the *BDF2* transcript generated through the HSP12 promoter (*$_p$HSP12-BDF2)* is cleaved by Rnt1p under this condition. We found that the *$_p$HSP12-BDF2* mRNA was still targeted by Rnt1p for rapid cleavage under salt stress (Figure 3D). In fact, the strong induction of the *HSP12* promoter under salt stress generated more transcripts to be targeted by RMD, resulting in a stronger accumulation of the cleavage fragment compared to wild type post-salt stress. RMD is also inadequate in cleaving all of the highly expressed *$_p$HSP12-BDF2* transcript, leading to some un-cleaved full-length transcripts. Nonetheless, our results indicate that the RMD hyper-activation on the *BDF2* transcript does not require *BDF2* natural promoter and/or the recruitment of Rnt1p to its natural promoter.

**Rnt1p cleavage stem loop identity influences RMD efficiency**

Previous studies have demonstrated that the identity of the Rnt1p recognition stem loop may affect cleavage efficiency of that transcript (Comeau et al., 2016). To further investigate how Rnt1p stem loop identity may affect RMD hyper-activation on *BDF2,* we replaced its Rnt1p cleavage stem loop to that of *UBP15's*, a transcript that contains a stem-loop that can be cleaved by Rnt1p *in vitro* (Figure 4B), but that does not undergo RMD hyper-activation in salt stress (Figure 4A). It is unclear whether the absence of RMD activity on *UPB15* transcript is due to the identity of its RCS or the localization of its transcript. Remarkably, the *BDF2* hybrid transcript containing the *UBP15* Rnt1p stem loop was no longer efficiently cleaved in either salt or ethanol stress conditions (Figure 4C and D), as a significant amount of the full length *BDF2* hybrid transcript was still detected after an hour of salt or ethanol treatment. To confirm that the RCS stemming from *UPB15* is folded properly within the context of the *BDF2* transcript, Rnt1p *in vitro* cleavage analysis was performed using purified Rnt1p. The Rnt1p *in vitro* cleavage of the *BDF2* hybrid transcript results in a complete loss of the full-length transcript, similar to that of the WT *BDF2* transcript. This indicates that the hybrid *BDF2* transcript can be indeed targeted and cleaved by Rnt1p. However, the rate of *in vitro* cleavage of the hybrid transcript is much slower than that of wild-type *BDF2* transcript (Figure 4E). This indicates that the results seen *in vivo* are not due to secondary effects caused from altering the *BDF2* sequence. Taken together, our data demonstrates that the Rnt1p cleavage efficiency of transcripts can indeed affect RMD activity during stress conditions.

**Discussion**

Bdf2p is a bromodomain protein involved in different aspects of transcription through its ability to recognize acetylated histones. We previously showed that the *BDF2* transcript is subject to both RMD and SMD pathways to limit and regulate its expression (Roy & Chanfreau, 2014). This is of particular importance during stress conditions, where a rewiring of transcription

and translation is necessary for cellular fitness. In high salt stress, an increase in activity of RMD on *BDF2* causes its transcript to become completely undetectable. This repression of *BDF2* is necessary for the robust expression of the stress responsive gene *GPH1,* and potentially other stress responsive genes as well (Roy & Chanfreau, 2014). Despite the significance of regulating the expression of *BDF2,* it is not known what triggers RMD hyperactivation during salt stress.

In this study, we demonstrate that the increase of RMD activity on *BDF2* in salt stress is not due to a direct change in the expression of Rnt1p or its localization within the cell. Rather, our study suggests that the nuclear retention of *BDF2* transcripts during stress conditions may cause the observed RMD hyperactivation. Blocking nuclear export of mRNAs, whether from stress conditions such as heat or ethanol shock, or by nuclear depletion of key export factors, can reproduce salt stress induced RMD hyperactivation on *BDF2* RNAs (Figure 2A and 3A-C). The RMD hyperactivation on *BDF2* RNAs is independent of the identity of the *BDF2* transcript promoter region, as switching its promoter to that of *HSP12* does not prevent RMD activity (Figure 3D). This suggests that the selective decay of RNA transcripts through a promoter dependent recruitment of Rnt1p does not play a role for *BDF2* transcripts in our conditions. Taken together, these results show that Rnt1p mediates the degradation of *BDF2* transcripts when mRNA export is blocked.

We further show evidence that the identity of the Rnt1p cleavage stem loop (RCS) within Rnt1p RNA substrates further influences their susceptibility to cleavage. This supports previous evidence that the nucleotide base pairing of the product termini can determine the Rnt1p substrate reactivity (Comeau et al., 2016). It is unclear whether certain stress conditions, such as heat shock or salt stress, may alter the structure of the RCS *in vivo* and influence its cleavage efficiency by Rnt1p. High temperatures may destabilize the RCS within the *BDF2* transcript and thereby decrease the efficiency of its cleavage. This may explain why the

cleavage activity of Rnt1p on the *BDF2* mRNA was not as robust in heat shock treatment as compared to ethanol or salt stress.

Altogether, our results indicate that Rnt1p may help regulate expression of specific genes through the cleavage and degradation of specific substrates based on their localization and stem loop structure. The nuclear export of many mRNAs is blocked during stress, which provides the opportunity for these mRNAs to be targeted by Rnt1p for degradation in these conditions. In fact, previous studies have shown that blocking the nuclear export of mRNAs results in the rapid degradation of newly synthesized RNAs (Tudek et al., 2018). It is possible that Rnt1p may play a role in this mechanism and more generally promote the removal of retained RNAs during stress.

## Materials and Methods

### Yeast strains

Unless otherwise noted, all strains used in this study were derived from BMA64 (Table S1). Strains were constructed using the lithium acetate/PEG/Single stranded carrier DNA transformation method (Gietz & Schiestl, 2007) with PCR products containing flanking regions of the area of interest for efficient homologous recombination. Mutations within the *BDF2* transcripts were constructed through the *delitto perfetto* approach (Storici & Resnick, 2006). Here, the Rnt1p target stem loop within the *BDF2* transcript (ChrIV:332367-80) was replaced with the CORE integration cassette, consisting of the *URA3* and *KanMX6* genes. Successful transformants were selected through their resistance to G418, and further confirmed through PCR. Afterwards, the CORE integration cassette was excised with various Rnt1p target stem loops using the transformation protocol as described above. Successful transformants were

selected on their ability to grow on 5-Fluoroorotic acid (5-FOA) due to the loss of *URA3* and confirmed through PCR and sanger sequencing (Laragen, Inc).

Anchor away strains were created in a modified HHY168 background (Haruki et al., 2008) where the *natMX6* marker was replaced with the *hphMX4* marker amplified from pAG32 (Goldstein & McCusker, 1999). The genes of interest were C-terminally tagged with the rapamycin binding domain (FRB) using the transformation method as described.

**Yeast media and growth conditions**

All strains were grown in YPD (1% yeast extract, 2% peptone, and 2% dextrose) at 30$^{o}$C unless noted otherwise. 50 mls of culture were harvested at $OD_{600}$ 0.4-0.6 by centrifugation at 4,000 rpm (Sigma Rotor11030) for 1.5 minutes before being transferred to 2ml screw capped Eppendorf tubes. The cells are then pelleted and flash frozen in liquid nitrogen immediately after the supernatant is removed. For anchor away experiments, cultures were grown to exponential phase before rapamycin (1mg/ml rapamycin dissolved in 90% ethanol and 10% tween 20) was added to a final concentration of 1ug/ml. The cultures are then grown for an additional hour before being harvested. For heat shift experiments, cells were grown to exponential phase at 23$^{o}$C before equal volumes of 61$^{o}$C preheated YPD were added to bring the temperature to 42$^{o}$C. The cultures are then harvested at the indicated times. For ethanol treatment, cells were grown to exponential phase before equal volumes of YPD or YPD containing 20% ethanol (v/v) were added, and then harvested at the indicated times.

**Yeast RNA extraction**

To the frozen cell pellets, 500 µL of phenol : chloroform : isoamyl alcohol (25:24:1, pH 6.7, OmniPur), 400 µL of acid-washed beads and 500 µL of RNA buffer (50 mM Tris-HCl pH 7.5, 100 mM NaCl, 10mM EDTA, 2% SDS w/v )were added and vortexed for 1 minute. The samples were then incubated at 65$^{o}$C for 6 minutes before being vortexed for another minute. Afterwards,

the samples were spun down at 13,200 rpm for 5 minutes before 450 µL of the aqueous layer was transferred to a new Eppendorf tube containing 450 µL of fresh phenol : chloroform : isoamyl alcohol. The mixture was vortexed for an additional hour before being spun down at 15,000 rpm for 2 minutes. About 400 µL of the top aqueous layer was transferred to a new Eppendorf tube containing 1ml of 100% ethanol and 40 µL of 3M sodium acetate pH 5.2. The samples were then cooled to -80$^{o}$C for 30 minutes to facilitate precipitation of the RNA. The samples are then spun down for 10 minutes at 15,000 rpm to pellet the precipitated RNA. The supernatant was then removed and the RNA pellet washed with 200 µL of 70% ethanol. The clean RNA pellets were resuspended in 40-80 µL of nuclease-free water before being quantitated using the NanoDrop (Thermoscientific).

**Northern Blot Analysis**

5 µg of total RNA were normalized to the same volume among all of the samples. The RNA aliquots were carefully combined with 4 times its volume of glyoxal buffer [60% DMSO (Sigma-Aldrich), 20% glyoxal v/v (Sigma-Aldrich), 5% glycerol, 40 µg/ml ethidium bromide, 1X BPTE pH 6.5 (10 mM PIPES (Sigma-Aldrich), 30 mM Bis-Tris (Sigma-Aldrich), 10 mM EDTA pH 8.0)] and incubated at 55$^{o}$C for 1 hour. The samples are then cooled on ice for an additional 5 minutes before being loaded onto 1.8% agarose gels made with 1X BPTE buffer. Electrophoresis was performed with 1X BPTE running buffer at 120V for 3-5 hours. During this time, the running buffer is constantly mixed with stir bars. After sufficient separation, the gel is washed with deionized water for 10 minutes, 75mM NaOH for 15 minutes, and in 1X BPTE buffer for 10 minutes. The RNA was then transferred overnight from the agarose gel to an Amersham Hybond-N$^{+}$ membrane (GE Healthcare Life Sciences) using 10X SSPE (100 mM sodium phosphate, 1.5 M NaCl, and 100 mM EDTA, pH 7.4). All membranes are cross-linked with Stratalinker UV Crosslinker 2400 (Stratagene) and if necessary, stored in 2X SSPE buffer at 4$^{o}$C. The membranes are pre-hybridized in Church's buffer (1% BSA w/v, 1mM EDTA, 0.5M

sodium phosphate pH 7.2, 7% SDS v/w) at 65°C for 1 hour before radiolabeled riboprobes are added directly into the buffer. The membranes are hybridized overnight before being washed twice with 2X SSPE, 0.1% SDS for 10 minutes each, and then twice with 0.1X SSPE, 0.1% SDS for 10 minutes each as well. For visualization, the washed blots are exposed to K-screens (Kodak) from several hours to up to 2 days depending on the strength of the signal. The screens are then scanned using the Bio-Rad FX Imager.

**Riboprobe synthesis for Northern blotting analysis**

Radiolabeled riboprobes were transcribed *in vitro* using T3 RNA polymerase (Promega) according to the manufacturers protocol. However, □-$^{32}$P-UTP (PerkinElmer) was used in lieu of □-$^{32}$P-CTP. The template used in the *in vitro* transcription were synthesized through PCR using primers corresponding to the gene of interest (Table S1). After synthesis, the riboprobes are directly transferred into hybridization bottles containing the pre-hybridized membranes.

***In vitro* Rnt1p cleavage assay**

Recombinant Rnt1p were purified as described previously (Henras et al., 2005). *In vitro* cleavage reactions were performed in 50 µL reactions consisting of 50 µg of total RNA, 10 pmol of purified recombinant Rnt1p, and 1X Rnt1p cleavage buffer (30 mM Tris pH 7.5, 150 mM KCl, 5 mM spermidine, 200 mM $MgCl_2$, 0.1 mM DTT, 0.1 mM EDTA). The reactions were incubated at 30°c and halted by the addition of 150 µL of RNA buffer at the times indicated. The reactions were then purified through using phenol-chloroform. Briefly, 200 µL of phenol : chloroform : isoamyl alcohol were added to the samples. The samples are vortexed for 1 minute and spun down for 2 minutes at 15,000 rpm. The top aqueous later were added to a fresh Eppendorf tube containing 1 ml ethanol, 40 µL 3M sodium acetate pH 5.2, and 1 µL of GlycoBlue (Ambion). Precipitation of the RNA were facilitated through incubating the samples at -80°c for 30 minutes

and then pelleted by centrifugation at 15,000 rpm for 10 minutes. The pellets were washed with 200 µL of 70% ethanol and resuspended in 15 µL of nuclease-free water.

**Figure legends**

**Figure 1**

**Rnt1p localization and protein abundance remains unchanged after salt stress. A**. Western blot analysis of Rnt1p. No differences in Rnt1p abundance levels were detected between strains treated with or without 0.6M NaCl stress. **B.** Nuclear localization of Rnt1p remains unchanged after salt treatment. A unique pattern in the localization of poly(A)+ mRNAs can be seen after salt treatment. GFP-tagged Rnt1p strains were treated with 0.6M NaCl stress and prepared for microscopy. Cy3 labeled oligo(dT) 50 were used to visualize poly(A)+ mRNAs. **C.** The nuclear depletion of Rnt1p prevents the cleavage of *BDF2* transcripts after salt stress.

**Figure 2**

**Stress induced nuclear export block of mRNAs induces RMD activity on *BDF2* transcripts. A-C.** Northern blot analysis showing RMD activity on the *BDF2* transcripts in various stress conditions. Both 10% ethanol and 42$^{o}$C heat shock induces RMD activity on *BDF2* transcripts, similar to 0.6M NaCl or LiCl stress. Strains are grown in standard growth conditions before being treated with the indicated stress. scR1 was used as a loading control.

**Figure 3**

**mRNA export block triggers RMD hyperactivation on *BDF2* RNAs. A-C.** Northern blot analysis indicating that the nuclear depletion of the CPA factors Nab2p, Nab4p, Yth1p and Ysh1p, and the mRNA export factor Mex67p results in robust activity of Rnt1p on *BDF2* RNA. Strains were grown in standard growth conditions before being treated with 0.6M NaCl, 1ug/uL Rapamycin or both for 1 hour. scR1 was used as a loading control. **D**. Northern blot analysis of

*BDF2* and *HSP12* RNAs. *BDF2* transcripts harboring the promoter of *HSP12* continue to be targeted for RMD hyperactivation in salt stress.

**Figure 4**

**Identity of RCS influences Rnt1p cleavage activity. A.** *UPB15* transcripts are a Rnt1p substrate that does not undergo RMD hyperactivation in salt stress. **B**. *In vitro* cleavage assay showing that *BDF2* transcripts containing the RCS of *UPB15* can be cleaved by Rnt1p. **C and D.** Northern blot analysis of *BDF2* transcripts harboring the RCS from *UPB15. BDF2* transcripts containing the RCS of *UPB15* display a decrease in the efficiency of cleavage in both salt and ethanol stress treatments. **E.** Rnt1p *in vitro* cleavage assay indicates a decrease in the rate of cleavage for the *BDF2* transcripts containing the RCS of *UPB15*

Figure 1

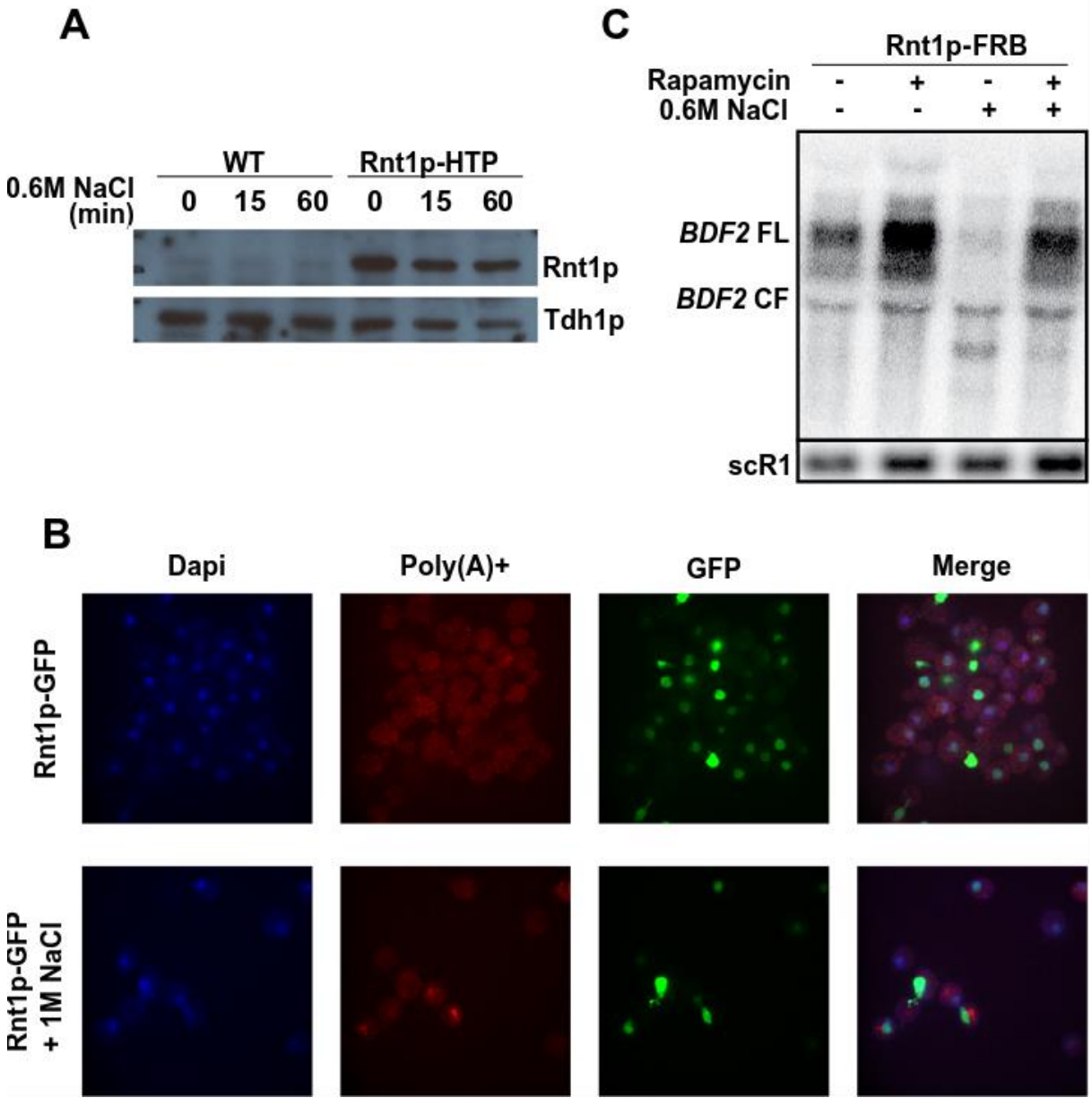
A
WT
Rnt1p-HTP
0.6M NaCl (min)
0
15
60
0
15
60
Rnt1p
Tdh1p
C
Rnt1p-FRB
Rapamycin
0.6M NaCl
BDF2 FL
BDF2 CF
scR1
B
Dapi
Poly(A)+
GFP
Merge
Rnt1p-GFP
Rnt1p-GFP + 1M NaCl

# Figure 2

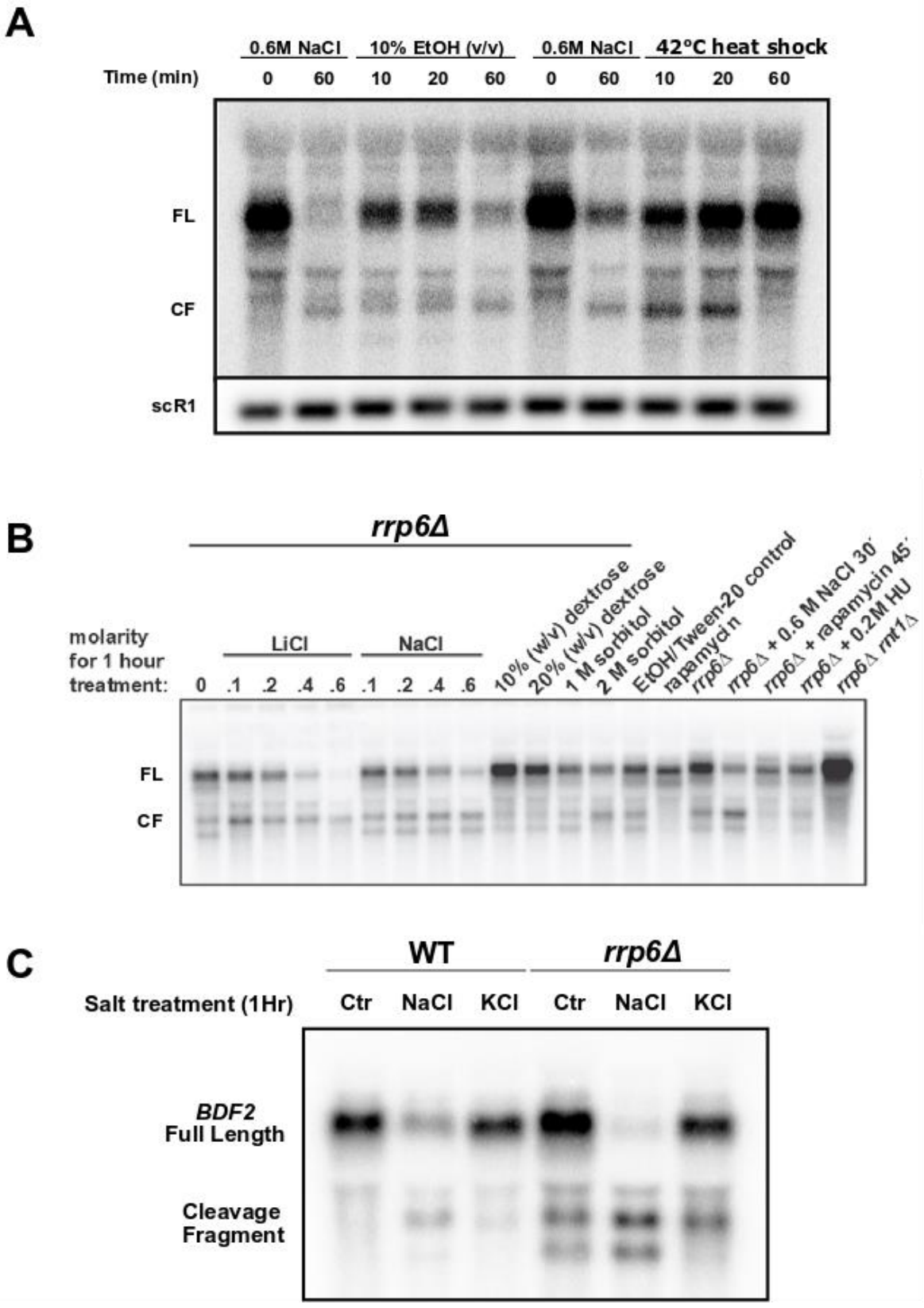
A
0.6M NaCl
10% EtOH (v/v)
0.6M NaCl
42°C heat shock
Time (min)
0 60 10 20 60 0 60 10 20 60
FL
CF
scR1
B
rrp6Δ
molarity for 1 hour treatment:
LiCl
NaCl
0 .1 .2 .4 .6 .1 .2 .4 .6
10% (w/v) dextrose
20% (w/v) dextrose
1 M sorbitol
2 M sorbitol
EtOH/Tween-20 control
rapamycin
rrp6Δ
rrp6Δ + 0.6 M NaCl 30'
rrp6Δ + rapamycin 45'
rrp6Δ + 0.2M HU
rrp6Δ rnt1Δ
FL
CF
C
WT
rrp6Δ
Salt treatment (1Hr)
Ctr NaCl KCl Ctr NaCl KCl
BDF2 Full Length
Cleavage Fragment

# Figure 3

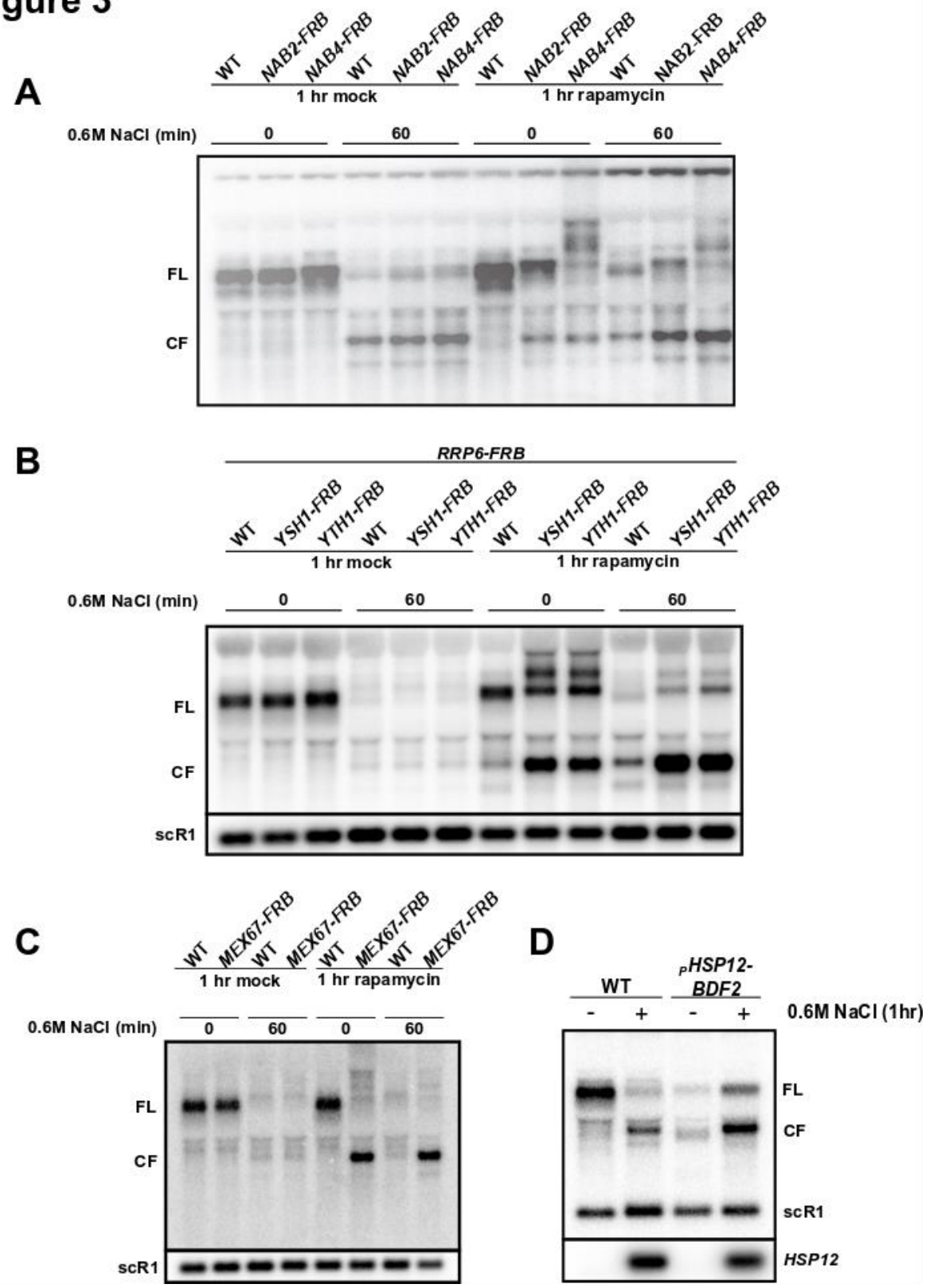
A
WT
NAB2-FRB
NAB4-FRB
1 hr mock
1 hr rapamycin
0.6M NaCl (min)
0
60
FL
CF
B
RRP6-FRB
YSH1-FRB
YTH1-FRB
scR1
C
MEX67-FRB
D
WT
pHSP12-BDF2
0.6M NaCl (1hr)
HSP12

# Figure 6

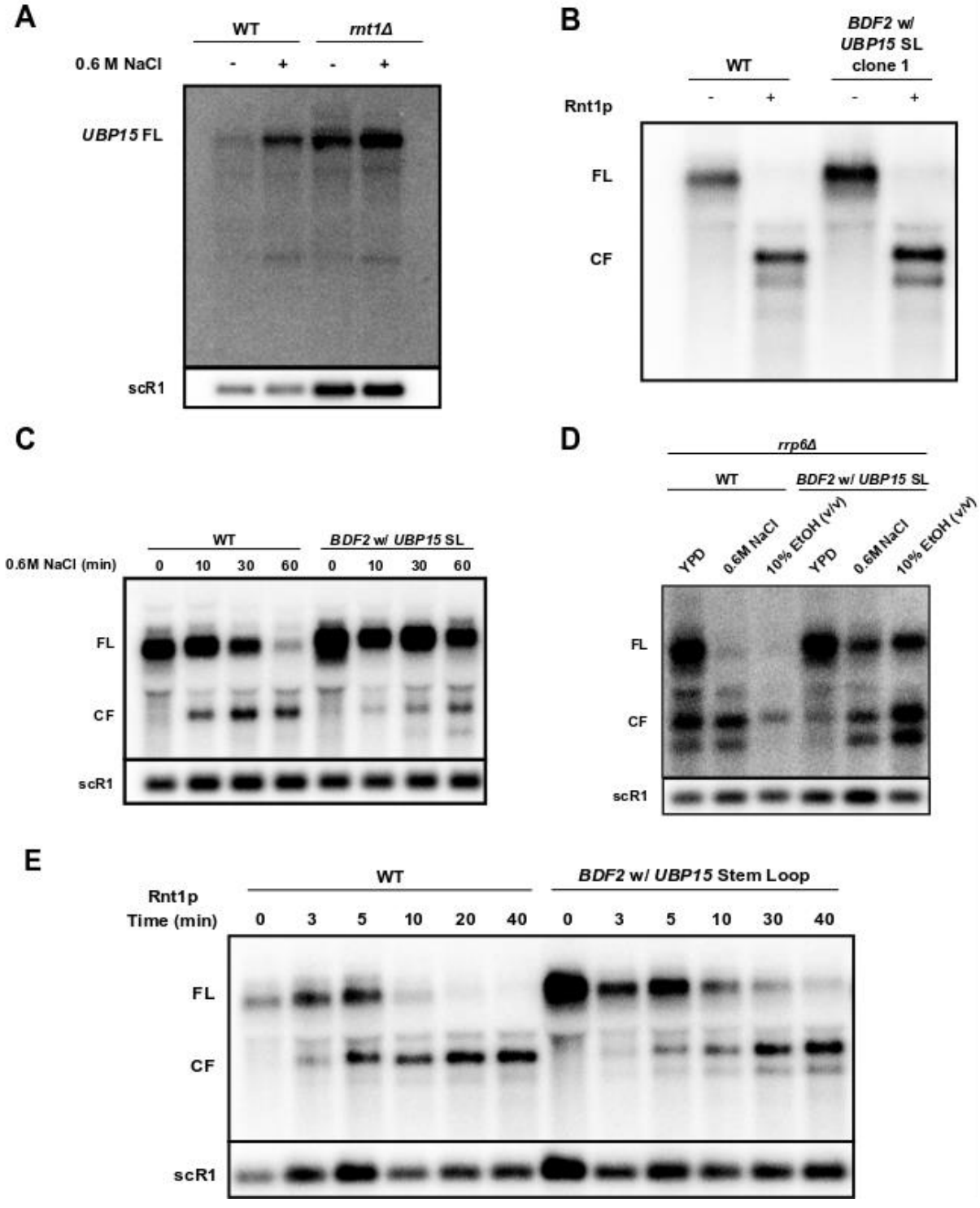
A
WT
rnt1Δ
0.6 M NaCl
- + - +
UBP15 FL
scR1
B
BDF2 w/ UBP15 SL clone 1
WT
Rnt1p
- + - +
FL
CF
C
WT
BDF2 w/ UBP15 SL
0.6M NaCl (min)
0 10 30 60 0 10 30 60
FL
CF
scR1
D
rrp6Δ
WT
BDF2 w/ UBP15 SL
YPD
0.6M NaCl
10% EtOH (v/v)
YPD
0.6M NaCl
10% EtOH (v/v)
FL
CF
scR1
E
WT
BDF2 w/ UBP15 Stem Loop
Rnt1p
Time (min)
0 3 5 10 20 40 0 3 5 10 30 40
FL
CF
scR1

**References**

Catala, M., & Abou Elela, S. (2019). Promoter-dependent nuclear RNA degradation ensures cell cycle-specific gene expression. *Communications Biology*, *2*(1), 211. https://doi.org/10.1038/s42003-019-0441-3

Catala, M., Lamontagne, B., Larose, S., Ghazal, G., & Elela, S. A. (2004). Cell Cycle-dependent Nuclear Localization of Yeast RNase III Is Required for Efficient Cell Division. *Molecular Biology of the Cell*, *15*(7), 3015–3030. https://doi.org/10.1091/mbc.e04-03-0183

Comeau, M.-A., Lafontaine, D. A., & Abou Elela, S. (2016). The catalytic efficiency of yeast ribonuclease III depends on substrate specific product release rate. *Nucleic Acids Research*, *44*(16), 7911–7921. https://doi.org/10.1093/nar/gkw507

Durant, M., & Pugh, B. F. (2007). NuA4-directed chromatin transactions throughout the Saccharomyces cerevisiae genome. *Molecular and Cellular Biology*, *27*(15), 5327–5335. https://doi.org/10.1128/MCB.00468-07

Fu, J., Hou, J., Liu, L., Chen, L., Wang, M., Shen, Y., Zhang, Z., & Bao, X. (2013). Interplay between BDF1 and BDF2 and their roles in regulating the yeast salt stress response. *FEBS Journal*, *280*(9), 1991–2001. https://doi.org/10.1111/febs.12219

Gietz, R. D., & Schiestl, R. H. (2007). High-efficiency yeast transformation using the LiAc/SS carrier DNA/PEG method. *Nature Protocols*, *2*(1), 31–34. https://doi.org/10.1038/nprot.2007.13

Goldstein, A. L., & McCusker, J. H. (1999). Three new dominant drug resistance cassettes for gene disruption in Saccharomyces cerevisiae. *Yeast (Chichester, England)*, *15*(14), 1541–1553. https://doi.org/10.1002/(SICI)1097-0061(199910)15:14<1541::AID-YEA476>3.0.CO;2-K

Guisbert, K. K., Duncan, K., Li, H., & Guthrie, C. (n.d.). *Functional specificity of shuttling hnRNPs revealed by genome-wide analysis of their RNA binding profiles*.

https://doi.org/10.1261/rna.7234205

Hammell, C. M., Gross, S., Zenklusen, D., Heath, C. V., Stutz, F., Moore, C., & Cole, C. N. (2002). Coupling of Termination, 3' Processing, and mRNA Export. *Molecular and Cellular Biology*, *22*(18), 6441–6457. https://doi.org/10.1128/MCB.22.18.6441-6457.2002

Haruki, H., Nishikawa, J., & Laemmli, U. K. (2008). The anchor-away technique: rapid, conditional establishment of yeast mutant phenotypes. *Molecular Cell*, *31*(6), 925–932. https://doi.org/10.1016/j.molcel.2008.07.020

Henras, A. K., Bertrand, E., & Chanfreau, G. (2004). A cotranscriptional model for 3'-end processing of the Saccharomyces cerevisiae pre-ribosomal RNA precursor. *RNA (New York, N.Y.)*, *10*(10), 1572–1585. https://doi.org/10.1261/rna.7750804

Henras, A. K., Sam, M., Hiley, S. L., Wu, H., Hughes, T. R., Feigon, J., & Chanfreau, G. F. (2005). Biochemical and genomic analysis of substrate recognition by the double-stranded RNA binding domain of yeast RNase III. *RNA (New York, N.Y.)*, *11*(8), 1225–1237. https://doi.org/10.1261/rna.2760705

Izawa, S., Kita, T., Ikeda, K., Inoue, Y., Piper, P., Tani, T., Derby, R. J., Hiraoka, Y., Spector, D. L., Saavedra, C., Tung, K. S., Amberg, D. C., Hopper, A. K., Cole, C. N., Sorger, P. K., Saavedra, C. A., Hammell, C. M., Heath, C. V., Cole, C. N., … Compagno, C. (2008). Heat shock and ethanol stress provoke distinctly different responses in 3′-processing and nuclear export of *HSP* mRNA in *Saccharomyces cerevisiae*. *Biochemical Journal*, *414*(1), 111–119. https://doi.org/10.1042/BJ20071567

Josling, G. A., Selvarajah, S. A., Petter, M., & Duffy, M. F. (2012). The role of bromodomain proteins in regulating gene expression. *Genes*, *3*(2), 320–343. https://doi.org/10.3390/genes3020320

Kurdistani, S. K., & Grunstein, M. (2003). Histone acetylation and deacetylation in yeast. In *Nature Reviews Molecular Cell Biology* (Vol. 4, Issue 4, pp. 276–284). https://doi.org/10.1038/nrm1075

Lawrence, M., Daujat, S., & Schneider, R. (2016). Lateral Thinking: How Histone Modifications Regulate Gene Expression. *Trends in Genetics*, *32*, 42–56. https://doi.org/10.1016/j.tig.2015.10.007

Matangkasombut, O., Buratowski, R. M., Swilling, N. W., & Buratowski, S. (2000). Bromodomain factor 1 corresponds to a missing piece of yeast TFIID. *Genes & Development*, *14*(8), 951–962. http://www.ncbi.nlm.nih.gov/pubmed/10783167

Minvielle-Sebastia, L., Beyer, K., Krecic, A. M., Hector, R. E., Swanson, M. S., & Keller, W. (1998). Control of cleavage site selection during mRNA 3' end formation by a yeast hnRNP. *EMBO Journal*, *17*(24), 7454–7468. https://doi.org/10.1093/emboj/17.24.7454

Nagy, Z., Comer, S., & Smolenski, A. (2018). Analysis of Protein Phosphorylation Using Phos-Tag Gels. *Current Protocols in Protein Science*, *93*(1), e64. https://doi.org/10.1002/cpps.64

Piper, P. W., Talreja, K., Panaretou, B., Moradas-Ferreira, P., Byrne, K., Praekelt, U. M., Meacock, P., Recnacq, M., & Boucherie, H. (1994). Induction of major heat-shock proteins of Saccharomyces cerevisiae, including plasma membrane Hsp30, by ethanol levels above a critical threshold. *Microbiology*, *140*(11), 3031–3038. https://doi.org/10.1099/13500872-140-11-3031

Piper, Peter W. (1995). The heat shock and ethanol stress responses of yeast exhibit extensive similarity and functional overlap. *FEMS Microbiology Letters*, *134*(2–3), 121–127. https://doi.org/10.1111/j.1574-6968.1995.tb07925.x

Roy, K., & Chanfreau, G. (2014). Stress-induced nuclear RNA degradation pathways regulate

yeast bromodomain factor 2 to promote cell survival. *PLoS Genetics*, *10*(9), e1004661. https://doi.org/10.1371/journal.pgen.1004661

Saavedra, C. A., Hammell, C. M., Heath, C. V., & Cole, C. N. (1997). Yeast heat shock mRNAs are exported through a distinct pathway defined by Rip1p. *Genes & Development*, *11*(21), 2845–2856. https://doi.org/10.1101/gad.11.21.2845

Saavedra, C., Tung, K. S., Amberg, D. C., Hopper, A. K., & Cole, C. N. (1996). *Regulation of mRNA export in response to stress in Saccharomyces cerevisiae. 10*(13). http://www.genesdev.org/cgi/doi/10.1101/gad.10.13.1608

Storici, F., & Resnick, M. A. (2006). The delitto perfetto approach to in vivo site-directed mutagenesis and chromosome rearrangements with synthetic oligonucleotides in yeast. *Methods in Enzymology*, *409*, 329–345. https://doi.org/10.1016/S0076-6879(05)09019-1

Trcek, T., Larson, D. R., Moldón, A., Query, C. C., & Singer, R. H. (2011). Single-molecule mRNA decay measurements reveal promoter- regulated mRNA stability in yeast. *Cell*, *147*(7), 1484–1497. https://doi.org/10.1016/j.cell.2011.11.051

Tudek, A., Schmid, M., Makaras, M., Barrass, J. D., Beggs, J. D., & Jensen, T. H. (2018). A Nuclear Export Block Triggers the Decay of Newly Synthesized Polyadenylated RNA. *Cell Reports*, *24*(9), 2457–2467. https://doi.org/10.1016/j.celrep.2018.07.103

Varela, J. O. C. S., Praekelt, U. M., Meacock, P. A., Planta, R. J., & Mager, W. H. (1995). The Saccharomyces cerevisiae HSP12 Gene Is Activated by the High-Osmolarity Glycerol Pathway and Negatively Regulated by Protein Kinase A. *MOLECULAR AND CELLULAR BIOLOGY*, *15*(11), 6232–6245. https://www.ncbi.nlm.nih.gov/pmc/articles/PMC230875/pdf/156232.pdf

Volanakis, A., Passoni, M., Hector, R. D., Shah, S., Kilchert, C., Granneman, S., & Vasiljeva, L. (2013). Spliceosome-mediated decay (SMD) regulates expression of nonintronic genes in

budding yeast. *Genes & Development*, *27*(18), 2025–2038.

https://doi.org/10.1101/gad.221960.113